Mesenchymal stem cell secretome decreases the inflammatory response in annulus fibrosus organ cultures

Journal:	*eCM Not-for-profit Open Access Journal*
Manuscript ID	Draft
Manuscript Type:	Disc Biology Special Issue
Date Submitted by the Author:	n/a
Complete List of Authors:	Neidlinger-Wilke, Cornelia; Ulm University, Institute of Orthopaedic Research and Biomechanics Ekkerlein, Andreas; Ulm University, Institute of Orthopaedic Research and Biomechanics Gonçalves, Raquel; Ulm University; Universidade do Porto Instituto de Investigação e Inovação em Saúde; Universidade do Porto Instituto de Ciências Biomédicas Abel Salazar Ferreira, Joana R.; Universidade do Porto Instituto de Investigacao e Inovacao em Saude, Microenvironments for NewTherapies Research Group; INEB, Microenvironments for NewTherapies Research Group; Universidade do Porto Instituto de Ciencias Biomedicas Abel Salazar Ignatius, Anita; Ulm University, Institute of Orthopaedic Research and Biomechanics Wilke, Hans-Joachim; Ulm University, Institute of Orthopaedic Research and Biomechanics Teixeira, Graciosa; Ulm University, Institute of Orthopaedic Research and Biomechanics
Keywords:	Intervertebral Disc - General, Intervertebral Disc - Degeneration, Intervertebral Disc - Herniation, Intervertebral Disc - Repair / Regeneration, Mechanical loading, Inflammation, Complement, Paracrine signalling
Abstract:	Mesenchymal stem/stromal cells (MSC)-based therapies have been proposed for back pain and disc degeneration, despite limited knowledge on their mechanism of action. The impact of MSC/their secretome on annulus fibrosus (AF) cells and tissue was analysed in bovine AF organ cultures (AF-OCs) exposed to upper-physiological cyclic tensile strain (CTS, 9 %, 1 Hz, 3 h/day) and interleukin (IL)-1β in a custom-made device. A 4-days treatment of the CTS+IL-1β stimulated AF-OCs with MSC secretome downregulated the expression of inflammation markers (*IL-6*, *IL-8*), complement system regulators (cluster of differentiation (*CD*)*46*, *CD55* and *CD59*) and metalloproteinases (*MMP-1*, *MMP-3*), but also of tissue inhibitors of metalloproteinases (*TIMP-1*, *TIMP-2*) and collagen type I. At protein level, it was confirmed that IL-6, MMP-3 and collagen content were decreased in the AF-OCs treated with the MSC secretome compared to the CTS+IL-1β stimulation alone. Nine days after treatment, a biomechanical peel-force test showed that the annular adhesive strength was significantly decreased by the MSC secretome treatment. Overall, MSC secretome had stronger impact on AF tissue

	than the MSC in co-culture. The secretome contributed to a decrease of the inflammatory and catabolic status of AF cells activated by CTS+IL-1β, and plays a role in the regulation of the complement system. However, it also contributed to a further decrease of collagen at gene/protein level and of the AF mechanical strength. Therefore, the use of MSC secretome as a therapeutic approach for disc-related diseases requires further mechanistic investigations before clinical trials.

Mesenchymal stem cell secretome decreases the inflammatory response in annulus fibrosus organ cultures

C. Neidlinger-Wilke[1#], A. Ekkerlein[1#], R. M. Goncalves[1-4], J. R. Ferreira[2-4], A. Ignatius[1], H.J. Wilke[1], G. Q. Teixeira[1*]

[1] Institute of Orthopaedic Research and Biomechanics, Trauma Research Centre, Ulm University, Ulm, Germany
[2] Instituto de Investigação e Inovação em Saúde (i3S), Universidade do Porto, Porto, Portugal
[3] Instituto de Engenharia Biomédica (INEB), Universidade do Porto, Porto, Portugal
[4] Instituto de Ciências Biomédicas Abel Salazar (ICBAS), Universidade do Porto, Porto, Portugal

[#] equal contribution

* **Corresponding author**:
Dr. Graciosa Quelhas Teixeira
Institute of Orthopaedic Research and Biomechanics
Trauma Research Centre
Ulm University
Helmholtzstraße 14, 89081 Ulm, Germany
Phone: +49-(0)731-500-55324
E-mail: graciosa.teixeira@uni-ulm.de

Running Title: *MSC secretome treatment of AF organ cultures*

Abstract

Mesenchymal stem/stromal cells (MSC)-based therapies have been proposed for back pain and disc degeneration, despite limited knowledge on their mechanism of action. The impact of MSC/their secretome on annulus fibrosus (AF) cells and tissue was analysed in bovine AF organ cultures (AF-OCs) exposed to upper-physiological cyclic tensile strain (CTS, 9 %, 1 Hz, 3 h/day) and interleukin (IL)-1β in a custom-made device. A 4-days treatment of the CTS+IL-1β stimulated AF-OCs with MSC secretome downregulated the expression of inflammation markers (*IL-6, IL-8*), complement system regulators (cluster of differentiation *(CD)46*, *CD55* and *CD59*) and metalloproteinases (*MMP-1, MMP-3*), but also of tissue inhibitors of metalloproteinases (*TIMP-1*, *TIMP-2*) and collagen type I. At protein level, it was confirmed that IL-6, MMP-3 and collagen content were decreased in the AF-OCs treated with the MSC secretome compared to the CTS+IL-1β stimulation alone. Nine days after treatment, a biomechanical peel-force test showed that the annular adhesive strength was significantly decreased by the MSC secretome treatment. Overall, MSC secretome had stronger impact on AF tissue than the MSC in co-culture. The secretome contributed to a decrease of the inflammatory and catabolic status of AF cells activated by CTS+IL-1β, and plays a role in the regulation of the complement system. However, it also contributed to a further decrease of collagen at gene/protein level and of the AF mechanical strength. Therefore, the use of MSC secretome as a therapeutic approach for disc-related diseases requires further mechanistic investigations before clinical trials.

Keywords: Intervertebral disc, degeneration, herniation, repair/regeneration, mechanical loading, inflammation, complement, paracrine signalling

Introduction

Intervertebral disc (IVD) degeneration and related inflammation are often associated with back, neck and radicular pain, major causes of disability worldwide that represent a large economic burden (Moradi-Lakeh *et al.*, 2017; Murray *et al.*, 2015). Current treatments ranging from physiotherapy to invasive surgeries, as spine fusion or IVD replacement, may decrease symptoms' progression but fail to restore the native IVD properties.

Though IVD degeneration can be linked with ageing (Roberts *et al.*, 2006), cases of early degeneration are often observed. The degenerative IVD pathogenesis may be caused by genetic predisposition, injury and/or lifestyle, among others. Disc degeneration involves the interplay between several mechanisms including mechanical overloading, catabolic cell response, degradation of matrix proteoglycans and loss of water-binding capacity (Adams and Roughley, 2006; Vergroesen *et al.*, 2015), as well as cell senescence and apoptosis (Roberts *et al.*, 2006). These events are often associated with an immune response, which plays an important role in the pathogenesis of IVD degeneration and cell death. During these events, production of extracellular matrix-degrading enzymes (metalloproteinase (MMP)-1, -3, -13, a disintegrin and metalloproteinase with thrombospondin motifs (ADAMTS)-4, -5, -13, etc.), proinflammatory mediators (interleukin (IL)-1β, -6, -8, tumour necrosis factor-α, etc.) and chemoattractants of immune cells (chemokine (C-C motif) ligand 2 (CCL2), CCL5) has been identified (Molinos *et al.*, 2015; Risbud and Shapiro, 2014). Complement-mediated processes are known coordinators of several events during inflammation, and significantly contribute to inflammation-mediated tissue damage (Ricklin and Lambris, 2013). Upon activation, complement proteins function as chemotactic factors and amplifiers of the inflammatory response (Ricklin and Lambris, 2013). The activation of the terminal complement complex (TCC) formation was shown to be abnormally high in human osteoarthritic joints (Wang *et al.*, 2011) and degenerated IVDs, with predominance in AF cells (Grönblad *et al.*, 2003). However, little is known about complement system regulation by IVD cells through the production of soluble complement factor H (CFH) or the expression of membrane-bound regulators including membrane cofactor protein (CD46), complement decay-accelerating factor (CD55) and protectin (CD59), which inhibits TCC formation and confers protection from complement-mediated lysis (Noris and Remuzzi, 2013).

Ultimately, the progressive structural weakening of the IVD may contribute to AF failure and tissue herniation (Adams and Roughley, 2006). The AF consists in concentric lamellae of regularly arranged collagen fibres, which are interconnected by a network of elastin and fibrillin as shown by Yu et al. (Yu *et al.*, 2015). The pathomechanism leading to the mechanical weakness of the AF and consequent disc herniation has not yet been described. Yet, the regenerative potential of the degenerated AF has been hypothesized to benefit from the presence of cells capable of proliferating and differentiating into AF-like cells. Although progenitor cells have been found in the human IVD, their number decreases very rapidly after birth (Sakai *et al.*, 2012), limiting IVD's potential to counteract degeneration or recover from an

injury. Therefore, cell-based therapies to stimulate IVD regeneration, namely those using bone marrow-derived mesenchymal stem/stromal cells (MSC), are being increasingly pursued. MSC transplantation potential has been linked to their ability to differentiate into IVD-like cells, producing IVD matrix components, or promoting stimulation of endogenous IVD cells, thus enabling anti-catabolic and anti-inflammatory effects, as reviewed by Sakai and Anderson (Sakai and Andersson, 2015). Patients have reported in clinical trials a reduction of pain after MSC transplantation; however, either no changes in the disc morphology or water binding capacity or only minor Pfirrmann grading improvement were observed (Noriega *et al.*, 2017; Orozco *et al.*, 2011; Yoshikawa *et al.*, 2010). MSC were shown to secrete anti-inflammatory factors, and influence matrix turnover, in short-term osteoarthritic synovium and cartilage explant cultures (van Buul *et al.*, 2012). Pereira *et al.* (Pereira *et al.*, 2016) has shown that MSC seeded on cartilaginous endplates significantly increased production of growth factors, as well as of collagen type II and aggrecan in IVD, namely in the NP. Cunha *et al.* (Cunha *et al.*, 2017) observed *in vivo*, in a rat disc herniation model, less degeneration/herniation for the MSC-transplanted group. Although no significant changes were detected in the extracellular matrix composition, the transplanted MSC seemed to modulate the immune response towards tissue regeneration (Cunha *et al.*, 2017). A previous study of our group showed that MSC in co-culture with a proinflammatory/degenerative nucleus pulposus (NP) organ culture can modulate the proinflammatory profile of the NP cells, while displaying themselves a proinflammatory profile (Teixeira *et al.*, 2018). However, because very few MSC have been found in the IVD tissue, we hypothesize that their paracrine effect *via* the secretome might have a larger effect on IVD cells that direct contact. MSC secrete numerous soluble factors in response to microenvironmental cues, regulating several mechanisms in neighbour tissues *via* paracrine signalling (Brisby *et al.*, 2013). Thus, several studies suggest the use of MSC secretome for cardiac tissue repair (Dai *et al.*, 2007), recovery of hepatic (Parekkadan *et al.*, 2007) and kidney (van Koppen *et al.*, 2012) functions, among others. Moreover, MSC secretome was suggested to stimulate IVD progenitor cells activity *ex vivo* in degenerated human IVD tissue samples toward the repair process (Brisby *et al.*, 2013). Hence, this work compared the therapeutic potential of not only MSC, but also their secretome to improve the understanding of the biochemical processes in the degenerative AF tissue using a standardized model. In that context, the following hypotheses were investigated: i) the proinflammatory environment leads to complement system activation and changes in AF cells phenotype and ii) MSC secretome is more effective in comparison to MSC transplantation to induce immune-mediated changes of AF tissue integrity.

Materials and Methods

MSC expansion and secretome production

MSC (Lonza) from human donors (n=3) were seeded at a density of 3000 cells/cm^2 and routinely expanded in MSC medium composed of low-glucose Dulbecco's Modified Eagle Medium (DMEM, Gibco) supplemented with 10 % HyClone foetal bovine serum (FBS; Thermo Scientific), 1 % Pen Strep (10,000 U/mL penicillin and 10,000 µg/mL streptomycin, Gibco) and 0.5 % amphotericin B (250 µg/mL, Gibco), at 37 °C and humidified atmosphere with 8.5 % CO_2. The medium was exchanged twice a week and cells were trypsinized when reaching 70% confluency.

For the secretome production, 10^6 MSC were seeded in 6-well plates (Corning) and incubated in 5 mL of MSC medium supplemented with 10 ng/mL recombinant human IL-1β (R&D Systems), at 37 °C and humidified atmosphere with 6 % O_2 and 8.5 % CO_2 for 2 days (Fig. 1a). Afterwards, the secretome was collected and centrifuged at 1800 g for 5 min, at 4°C, to remove cell debris, and then stored at -80 °C until further use. The MSC were harvested for gene expression analysis (Supplemental data). Cells kept under basal conditions were also collected for gene expression analysis prior to co-culture with AF-OCs. MSC in passage 4-9 were used for the experiments.

Tissue dissection and organ culture preparation

AF-organ cultures (AF-OCs) were prepared according to Saggese *et al.* (2019). Bovine tails from 12-24 months-old animals (n=20) were obtained from a local slaughterhouse (Fleischmarkt Donautal, Ulm) and dissected within 2 h after killing. Coccygeal segments 2-3 to 7-8 were isolated and the NP was removed using 14-16 mm diameter punches, depending on the IVD size. The collected AF rings were incubated with IVD medium composed of low-glucose DMEM supplemented with 5 % FBS Superior (Biochrom), 1 % non-essential amino acids (Biochrom), 1 % Pen Strep, 0.5 % amphotericin B and 1.5 % 5 M NaCl/0.4 M KCl solution to adjust osmolarity to 400 mOsm, at 37 °C and humidified atmosphere with 6 % O_2 and 8.5 % CO_2, as previously described (Neidlinger-Wilke *et al.*, 2012; Teixeira *et al.*, 2016). The rings were left for 6 days in 6-well plates (Corning) with membrane filter inserts (Millipore) and 0.46 MPa static loading (Teixeira *et al.*, 2016). The medium was exchanged every second day.

Treatment of AF rings with MSC and MSC secretome

On day 6, the AF-OCs were transferred to silicone dishes and placed in a cyclic tensile strain (CTS) device (Saggese *et al.*, 2019). The experimental timeline and groups are depicted in Fig. 1b.

For the AF-OCs treated with MSC co-culture, 10^6 MSC were seeded on top of the AF rings in the CTS device and left for 24 h to adhere. On the next day, the medium was exchanged in all experimental groups according to Table 1. The AF-OCs were stimulated with CTS at 1 Hz, 3 h per day. The CTS generated a 9 ± 3 % tensile stress of the AF-OC rings, representing a high physiological loading (Saggese *et al.*, 2019). One group was stimulated with CTS+IL-1β alone, an additional group was stimulated with

CTS+IL-1β and MSC were co-cultured on top of the AF rings. A third group was stimulated with CTS+IL-1β and the culture medium was mixed with MSC secretome. The MSC secretome was mixed in a 1:1 ratio with IVD medium before supplementation with 10 ng/mL IL-1β. Unstimulated AF rings were kept as control group.

At day 11, samples were collected for different analyses. The AF rings were separated into 3 sections: the tissue was either i) immediately shock frozen in RNAlater ICE (Invitrogen) and liquid nitrogen and stored at -80 °C for RNA isolation, ii) weighted (tissues with weight between 70 and 130 mg were collected) and then frozen at -20 °C for DNA and protein quantification or iii) used for metabolic activity quantification and afterwards fixed in 4 % phosphate-buffered formaldehyde solution for immunohistochemical staining.

For the AF-OCs that underwent treatment for 9 days, 50 % of the medium was exchanged at day 11 according to Table 1. At day 16, the AF rings were collected for metabolic activity quantification and mechanical testing. The supernatants were collected for protein quantification.

Metabolic activity of AF cells in organ culture

The metabolic activity of the AF cells was assessed by resazurin reduction assay. AF tissue sections of 70-130 mg wet weight were incubated with 0.02 mg/mL resazurin sodium salt (Sigma-Aldrich) solution in IVD medium. Samples were incubated for 2 h at 37 °C. Fluorescence intensity was measured in a spectrophotometer microplate reader (Tecan), with 530 nm excitation filters and 590 nm emission filters. Results were normalized to wet weight (mg) for each AF tissue. The AF tissues were frozen at -20 °C for protein quantification.

Gene expression analysis of AF cells

The tissues frozen in RNAlater ICE were thawed, the RNAlater was removed and 1 mL of TRIzol was added to the tissue to maintain the RNA integrity during tissue homogenization by a dismembrator (Miccra GmbH). Afterwards, 200 µL of chloroform were added to perform a two-phase extraction of the RNA. After a 5 min incubation step, the mixture was centrifuged at 14000 rpm and 4 °C for 30 min. The RNA was collected and transferred to an RNAse-free reaction tube. By adding an equivalent amount of 70 % EtOH, the RNA was precipitated. RNA isolation was performed using the MiraCol Purification Columns and the PicoPure RNA Isolation kit (ThermoFisher Scientific). For cDNA synthesis with integrated removal of DNA contamination, 12 µL of RNA were treated with the QuantiTect Reverse Transcription kit (ThermoFisher Scientific). Gene expression analysis was performed with primers for the reference gene bovine glyceraldehyde 3-phosphate dehydrogenase *(bGAPDH),* as well as for the target genes in Table 2. The transcribed cDNA was either mixed with custom-designed primers and the Platinum SYBR Green qPCR SuperMix-UDG kit (Invitrogen), or TaqMan Gene Expression Assays and Fast Advanced Master Mix (Applied Biosystems). The runs were performed in the QuantStudio 3 real-time PCR

system (Applied Biosystems). The melt curves were analysed to confirm the specificity of the reaction and quantification cycle (Cq) 35 cutoff was used. Relative expression levels were calculated using the Cq method ($\Delta Ct = Ct_{(gene\ of\ interest)} - Ct_{(GAPDH)}$), according to published guidelines (Bustin *et al.*, 2009).

Protein quantification in the organ culture supernatants

The concentration of PGE_2 (Arbor Assays), bovine IL-6 (bIL-6, MyBioSource), human IL-6 (hIL-6, BioLegend), hCFH (Abcam), hTIMP-1 and hTIMP-2 (RayBiotech) was measured by enzyme-linked immunosorbent assay (ELISA) in the supernatants at days 11 and 16 of organ culture.

DNA and protein quantification in the AF tissue

AF tissues were digested overnight at 56 °C with 0.5 mg/mL proteinase K (Sigma-Aldrich) solution for DNA and sulfated glycosaminoglycan (sGAG) quantification. DNA content was measured using the PicoGreen dsDNA assay kit (Invitrogen). sGAG content was determined using the Blyscan assay kit (Biocolor). AF tissues were digested for soluble collagen and elastin quantification according to the Sircol and the Fastin assay kits, respectively (Biocolor).

Immunohistochemistry

After fixation in formalin for 48 h, the AF samples were washed under running tap water for 2 h, dehydrated and embedded in paraffin. Cross-sections with 7 µm thickness were dewaxed and rehydrated. For antigen retrieval, the sections were incubated with 10 mM citrate buffer (pH 6.0, 85 °C, 20min), followed by hyaluronidase (2 mg/mL in citrate buffer, pH 8.0, 30 min, 37 °C) and collagenase (2 mg/mL in citrate buffer, pH 8.0, 15 min, 37 °C) digestion. Avidin–biotin complex kit (PK-6100, Vector laboratories) and NovaRED Peroxidase (HRP) Substrate kit (SK-4800, Vector Laboratories) were used for the immunostaining. Sections were incubated with rabbit anti-IL-6 (1:200 dilution, Bioss) or rabbit anti-MMP3 (1:200, Abcam) antibodies, overnight at 4 °C. Goat anti-rabbit IgG Biotin-XX (1:200 dilution, Invitrogen) was used as secondary antibody. All samples from the same experiment were stained at the same time for each marker for comparison purposes.

Microscopy and image analysis

From each of the IL-6 and MMP-3 stained sections, pictures were collected from three different areas. For each area, images were taken using bright-field and polarized-light microscopy and 5x magnification. Polarized-light images were used to distinguish the birefringent lamella matrix (LM) from the black translamellar bridging network (TLBN) regions. To evaluate each staining, the bright-field images were processed using ImageJ software and the colour deconvolution function to separate the NovaRED and Haematoxylin colour components. Then, the TLBN and the LM were outlined in the Nova Red colour channel as regions of interest and the average pixel intensity was measured for each region. The TLBN/LM ratio of the colour intensities

was calculated and the average of the three images was used to normalize the values of each sample to the control sample from the same experiment. For each experiment (n = 7-10) all samples were stained at the same time.

Mechanical testing

A peel test was performed to determine the peeling strength of the AF, according to Gregory *et al.* (Gregory *et al.*, 2012). AF segments were incised along a central lamella by 5 mm into a "Y" configuration. The split ends of the specimens were fixed in a "T" configuration in a uniaxial material testing machine (Zwick). The adjacent lamellae were pulled apart at 0.5 mm/s until they complete separation of the tissue. The average force in the plateau regions of each force-displacement curve was normalized to the height of the AF tissue and used to calculate the delamination strength (Gregory *et al.*, 2012; Saggese *et al.*, 2019)

Statistical analysis

Results are presented as median ± interquartile range. Statistical analysis was performed using GraphPad Prism 8 software (GraphPad Software, Inc., La Jolla, CA, USA). Data normal distribution was tested using D'Agostino–Pearson omnibus normality test. Parametric data were analysed using unpaired *t*-test to determine differences between two groups or one-way ANOVA to determine differences between three or more groups. Nonparametric data were analysed using Kruskal–Wallis test with Dunn's multiple comparison test to determine differences between three or more groups. Significance was set at $p < 0.05$.

Results

Analysis of cell viability and gene expression profile of AF cells

To induce a degenerative and proinflammatory environment, AF-OCs were stimulated at day 7 after isolation with CTS+IL-1β. The rings were either treated with MSC (MSC group) or secretome of pre-conditioned MSC (secretome group) to mimic the physiological conditions of MSC in the AF-OC model. The unstimulated and pre-conditioned MSC were analysed for gene expression of different human markers such as inflammation cytokines (*hIL-6*, *hIL-8*), matrix degrading enzymes (*hMMP-1*, *hMMP-3*), complement components (*hC3*, *hC5*, *hC6*, *hC7*, *hC8A*, *hC9*) and complement regulators (*hCD46*, *hCD55*, *hCD59)* (Supplemental data, Fig. 9).

To investigate whether AF cell viability was affected by the CTS+IL-1β conditions, co-culture with MSC or secretome treatment after 4 days of organ culture, mitochondrial metabolic activity and the expression of *bNOS2*, a marker of cell survival, were analysed (Fig. 1a,b). No differences were observed between the experimental groups. The proinflammatory markers *bIL-6* ($p < 0.01$), *bIL-8* ($p < 0.05$), *bPTGS2* ($p < 0.01$) and the inhibitory complement receptor *bCD46* ($p < 0.05$) were significantly upregulated in the group treated with CTS+IL-1β in comparison to the control (Fig. 1c). The secretome treatment significantly downregulated the expression of *bIL-6* ($p < 0.05$), *bIL-8* ($p < 0.05$),

CD46 ($p < 0.01$), CD55 ($p < 0.05$) and CD59 ($p < 0.001$) *versus* the CTS+IL-1β stimulation alone. *bIL-8* gene expression was also downregulated in the co-culture with MSC ($p < 0.05$). *bPTGS2*, responsible for production of inflammatory prostaglandins, was not affected in the MSC or secretome groups.

The main AF matrix components *bCOL1A1* and *bACAN*, inhibitors of matrix degradation *bTIMP-1* and *bTIMP*-2, as well as matrix degrading enzymes *bMMP-1*, *bMMP-3*, *bADAMTS-4* and vascularization marker *bVEGF* were also analysed by gene expression (Fig. 3). While *bACAN* expression was not altered in the different groups, *bCOL1A1* was downregulated in the MSC and secretome groups *versus* CTS+IL-1β ($p < 0.001$, Fig. 3a); *bTIMP-1* and *bTIMP*-2 were also significantly downregulated by the secretome ($p < 0.001$, Fig. 3b). *bMMP-1*, *bMMP-3* and *bADAMTS-4* were upregulated by the CTS+IL-1β stimulation, when compared to Control ($p < 0.01$, Fig. 3c), but downregulated by the combination with the secretome treatment ($p < 0.05$). Although not significant, *bVEGF* expression was slightly upregulated with the secretome treatment in comparison to the Control and CTS+IL-1β groups.

AF matrix remodelling

After 4 days of stimulation, no differences were found in the DNA content released to the culture supernatant between CTS+IL-1β and Control (Fig. 4a); however, the group treated with MSC ($p < 0.0001$) or secretome ($p < 0.05$) showed an increase in the DNA released to the culture supernatant. When the DNA content was quantified in the AF tissue itself, no differences were detected between the groups (Fig. 4b). Collagen, elastin and sGAG matrix components were also quantified in the AF tissue (Fig. 4c). Elastin and sGAG content were similar in all the conditions, but the collagen content was lower in the groups treated with MSC ($p = 0.05$) or secretome ($p < 0.05$) in contrast with the CTS+IL-1β stimulation alone, which was in agreement with the gene expression results for *bCOL1A1*.

Production of soluble factors

The distribution of IL-6 and MMP-3 in the AF tissue was assessed by immunohistochemistry at day 11 (Fig. 5). IL-6 and MMP-3 were distributed all over the AF tissue (Fig. 5a). For IL-6, a significantly higher staining intensity was found in the CTS+IL-1β group in comparison to the Control ($p < 0.01$, Fig. 5b) and to the secretome treatment ($p < 0.01$). A significantly higher staining intensity was also found for MMP3 in the CTS+IL-1β stimulation alone in contrast to the secretome treatment ($p < 0.01$, Fig. 5c).

PGE_2, bIL-6, hIL-6, hCFH, hTIMP-1 and hTIMP-2 content in the AF-OC supernatants was quantified after 4 days of stimulation and treatment (Fig. 6). PGE_2 production was higher in the CTS+IL-1β-stimulated group *versus* Control samples ($p < 0.05$, Fig. 6a), as previously observed (Saggese *et al.*, 2019), but no significant changes were detected with the MSC-based treatments. Interestingly, bIL-6 production was also higher with the CTS+IL-1β stimulation ($p < 0.05$, Fig. 6b), but this production was decreased by the co-culture with MSC ($p < 0.05$). hIL-6, hCFH, hTIMP-1 and hTIMP-2 were only detected

in the supernatants from MSC- and secretome-treated groups, indicating that the assays detected specifically the molecules produced by human MSC (Fig. 6c-e). Higher hIL-6, hCFH, hTIMP-1 and hTIMP-2 were found in the secretome group *versus* the group treated with MSC in co-culture ($p < 0.0001$).

After 9 days of stimulation and treatment (day 16), it was observed significantly lower mitochondrial metabolic activity in CTS+IL-1β group ($p < 0.05$, Fig. 7a), which was recovered with the secretome treatment ($p < 0.05$). Similarly to what was observed after 4 days of stimulation/treatment (day 11), higher PGE_2 ($p < 0.05$, Fig. 7b) and bIL-6 ($p < 0.05$, Fig. 7c) release to the supernatant were measured in CTS+IL-1β *versus* Control. The MSC co-culture with the AF-OCs significantly decreased the production of bIL-6 in comparison to the CTS+IL-1β stimulation alone ($p < 0.05$). hIL-6, hCFH and hTIMP-2 content in the supernatant was significantly higher in the secretome-treated group in comparison to the release by the MSC in direct co-culture with the AF-OCs ($p < 0.01$, Fig. 7d-f).

Mechanical properties of AF tissue

A biomechanical peel test was performed in AF tissue segments after 9 days of organ culture stimulation/treatment (Fig. 8). Force-displacement curves were obtained and the mean force along one or more plateau regions was used to calculate the average annular delamination strength for each sample. Interestingly, the CTS+IL-1β did not display differences in comparison to the Control group as expected following the results from Saggese *et al.* (2019) after 5 days of AF-OC stimulation. However, about 30% lower delamination strength was found in the groups treated with MSC ($p = 0.07$). and secretome ($p < 0.05$) compared to the CTS+IL-1β stimulation alone, in line with the lower collagen expression/production observed in the MSC and secretome groups.

Discussion

The healthy IVD is characterised by a harsh microenvironment, due to low oxygen levels, high osmolarity, nutritional deficits and high mechanical loading, and these conditions are further aggravated by degeneration and inflammation (Molinos *et al.*, 2015; Urban, 2002). The proinflammatory/degenerative microenvironment, particularly low oxygen (5% O_2) and low glucose (1 mM glucose) conditions have been shown to promote stem cell death, and to inhibit proliferation and sGAG and collagen production *in vitro* (Naqvi and Buckley, 2015). Acidic pH conditions have also been found to impair the survival and function of stem cells (Naqvi and Buckley, 2016; Wuertz *et al.*, 2009). In the present study, the proinflammatory and catabolic environment of the IVD was simulated using a previously established *ex vivo* model of bovine AF rings cultured under low oxygen and low glucose supply, iso-osmotic (400 mOsm) conditions and CTS+IL-1β stimulation (Saggese *et al.*, 2019). This model was characterized by an increased production of cyclooxigenase-2 (COX-2), PGE_2, IL-6 and MMP-3, as well as a decrease in the annular peel strength in comparison to non-stimulated controls (Saggese *et al.*, 2019). The proinflammatory/degenerative

conditions were replicated in the current study with a longer investigation period of up to 9 days. An increased expression/production of proinflammatory cytokines and matrix degrading enzymes was observed after CTS+IL-1β stimulation. These results are supported by previous studies which showed activation of an inflammatory and catabolic reaction by human AF and NP cells exposed to high mechanical strain (Gawri *et al.*, 2014; Gilbert *et al.*, 2010; Pratsinis *et al.*, 2016). Interestingly, no changes were observed regarding the expression of membrane-bound regulatory proteins *bCD46*, *bCD55* and *bCD59* (important for the protection of the cells against complement-mediated lysis) with CTS+IL-1β stimulation. IL-1β stimulation alone of isolated human articular chondrocytes has been previously described to induce upregulation of complement regulators CD45, CD55 and CD59 (Hyc *et al.*, 2003). Nevertheless, a synergistic interplay between IL-1β and C3a or C5a was suggested to regulated the release of IL-6 by isolated osteoblasts and to up-regulate RANKL/OPG expression (Ignatius *et al.*, 2011). There results suggest that complement activation may enhance the inflammatory response especially in a pro-inflammatory environment.

In our CTS+IL-1β-stimulated AF-OCs, no changes in aggrecan expression, collagen, elastin or sGAG matrix content were detected in comparison to non-stimulated tissues. Though the AF matrix is composed of other proteins that might have been targeted (Melrose *et al.*, 2008), fibrillin was also shown not to be altered by this model after 5 days of stimulation, and the decrease in annular strength previously observed (Saggese *et al.*, 2019) seemed to have recovered after 9 days, as shown here. To more closely simulate the human physiological conditions and induce matrix breakdown and annular tear, a model using higher strains and complex loading (Heuer *et al.*, 2008) could be used in the future.

MSC-based therapies have been investigated for IVD regeneration and back pain treatment due to MSC's ability to differentiate in response to the microenvironment and cell-cell interaction into an NP-like phenotype, promoting matrix synthesis (Strassburg *et al.*, 2010), and to their anti-inflammatory and immune-modulatory activity (Cunha *et al.*, 2017; Miguélez-Rivera *et al.*, 2018; Teixeira *et al.*, 2018). Clinical trials have shown an increase in the IVD water content and an improvement of pain and disability in up to 2 years of follow-up (Noriega *et al.*, 2017; Orozco *et al.*, 2011; Pettine *et al.*, 2016; Pettine *et al.*, 2015; Yoshikawa *et al.*, 2010). These therapies have been mostly focused on restoring extracellular matrix production (particularly aggrecan) due to its impact on disc biomechanics (Adams and Roughley, 2006; Bendtsen *et al.*, 2016), but still little is known regarding the biological effects of MSC transplantation. Moreover, few studies have addressed/targeted a functional AF repair (Sakai and Grad, 2015).

In a previous study, MSC were cultured on top of punctured bovine IVD tissues under stimulation with low oxygen and low glucose supply, IL-1β medium supplementation and iso-osmotic (400 mOsm) conditions for 2 days (Teixeira *et al.*, 2018). The MSC in co-culture induced a downregulation of proinflammatory markers *IL-6* and *IL-8* by the disc cells; however, without an effect on ECM remodelling (Teixeira *et al.*, 2018). The study also showed that while the IVD cells displayed a less proinflammatory

phenotype, the MSC produce higher amounts of the proinflammatory molecules IL-6, IL-8 and PGE_2, which suggested an MSC mechanism-of-action dependent on a cytokine feedback loop (Teixeira *et al.*, 2018).

MSC secrete numerous soluble factors in response to the microenvironmental cues, tuning several mechanisms in neighbor tissues via paracrine signaling (Ferreira *et al.*, 2018). Thus, the therapeutic potential of MSC secretome has been investigated in the context of several disorders, including degenerative joint diseases (Ferreira et al., 2018). MSC secretome has been suggested to stimulate IVD progenitor cells activity in human degenerated IVD tissues toward repair (Brisby *et al.*, 2013). Nonetheless, the MSC secretome content may be determined by the microenvironment to which the cells are exposed (Ferreira *et al.*, 2018). Hence, the effect of MSC *versus* pre-conditioned MSC secretome was evaluated in this work.

The MSC were exposed to low oxygen atmosphere (6% O_2) and proinflammatory stimulus (IL-1β medium supplementation), features of the AF-OC microenvironment. The pre-conditioned MSC displayed upregulated expression of proinflammatory markers *IL-6* and *IL-8*, and matrix degrading enzymes *MMP-1* and *MMP-3* (Supplemental data). Preconditioning of MSC ex vivo by low oxygen atmosphere, inflammatory stimulus, among others, prior to their use in therapy is recognized as an adaptive strategy that tunes the cells to survive in harsh microenvironments and enhances their regulatory function of the innate and adaptive immune responses (Saparov *et al.*, 2016). MSC-mediated immunomodulation has mainly been attributed to paracrine mechanisms associated with secretion of proinflammatory/ immunoregulatory mediators (Krampera *et al.*, 2006; Ren *et al.*, 2008). Nonetheless, the presence of different concentrations of proinflammatory molecules may influence differently MSC immunomodulatory response (Li et al., 2012), which suggests that just the use of the secretome may lead to a more reproducible outcome. Particularly MSC IL-1β-preconditioning has been shown to significantly upregulate the expression of multiple cytokines such as COX-2, TNF-α, IL-6, IL-8 and IL-23A, chemokines including CCL5, CCL20, CXCL1, CXCL3, CXCL5, CXCL6, CXCL10, and CXCL11, as well as adhesion molecules VCAM-1, ICAM-1, and ICAM-4 expression compared with non-stimulated MSC (Carrero *et al.*, 2012; Fan *et al.*, 2012). IL-1β preconditioning has also been described, for instance, to improve MSC ability to migrate to the spleen, mesenteric lymph nodes, and colon in a murine experimental model of colitis, and contributed to the reduction of the number of M1 macrophages in the peritoneal cavity (Fan *et al.*, 2012). Moreover, even though IL-1β-stimulated MSC in co-culture with IVD tissue presented a proinflammatory phenotype, producing high amounts of IL-6 and IL-8, the expression of these factors by the IVD cells was downregulated in response (Teixeira *et al.*, 2018). Complement *C3* and *C5* and regulatory proteins *CD46*, *CD55* and *CD59* were also shown to be upregulated by the pre-conditioned MSC, whereas TCC components *C6* and *C9* were downregulated in comparison to MSC cultured under atmospheric oxygen conditions and normal expansion medium (Supplemental data), indicating a preferably active production of anaphylatoxins instead of TCC. MSC were previously described to constitutively secrete CFH, a first line of complement

inhibition (Tu *et al.*, 2010). Ignatius et al. (Ignatius *et al.*, 2011) showed that human MSC express *C3*, *C5*, but also *CD46*, *CD55*, and *CD59*, allowing the inhibition of the complement system activation to a certain extent. Soluble MSC have also been shown to express central complement receptors for anaphylatoxins C3a and C5a (Ignatius *et al.*, 2011; Soland *et al.*, 2013), and these receptors were shown to contribute to the recruitment of MSC to sites of injury MSC are recruited and activated by anaphylatoxins after transplantation, potentially causing MSC death and limiting therapeutic benefit (Soland *et al.*, 2013).

As mentioned above, this study investigated the effect of MSC *versus* pre-conditioned MSC secretome on AF-OCs. After 4 days of culture, cell metabolic activity and *bNOS2* gene expression indicated a similar cell survival up to this point. *bNOS2* encodes a nitric oxide synthase which is inducible by a combination of lipopolysaccharide and proinflammatory cytokines, such as IL-1α (Kohyama *et al.*, 2000). Nonetheless, after 9 days of AF-OC, a decrease in mitochondrial metabolic activity was observed for the CTS+IL-1β group, which was only recovered in the secretome-treated group. IVD cell apoptosis has been associated with disc degeneration (Kohyama *et al.*, 2000). MSC-conditioned medium was previously shown to reduce nitric oxide production in cartilage explants (van Buul *et al.*, 2012). Cheng et al. (Cheng *et al.*, 2018) provided evidence that NP cell apoptosis and intervertebral disc degeneration can be decreased *in vivo*, in a rat model, by MSC-secreted exosomes, and therefore confirming MSC paracrine effects.

A paracrine immunomodulatory effect of MSC secretome has been described in osteoarthritic cartilage explant cultures (van Buul *et al.*, 2012) and it was also confirmed in the present study in AF cultures. We observed a decrease in the expression of *bIL-6* and *bIL-8*, as well as of *bCD46*, *bCD55* and *bCD59* by AF cells in presence of pre-conditioned MSC secretome. Because barely any differences were observed in the group with MSC in co-culture and the hIL-6, hCFH, hTIMP-1 and hTIMP-2 supernatant content was significantly lower in the group treated with MSC in co-culture than with the secretome, it might indicate low MSC adherence to the AF tissue, as shown by the DNA quantification in the supernatant. Interestingly, in our experiments, *bPTGS2* expression and overall PGE_2 production did not seem to be altered by the MSC or secretome treatments in comparison to CTS-IL-1β stimulation alone. PGE_2 is an important molecule that converts proinflammatory M1 macrophages into anti-inflammatory M2 macrophages at it has been shown to be highly produced by MSC and IVD cells in co-culture with IL-1β stimulation (Teixeira *et al.*, 2018). A study by Miguélez-Rivera and colleagues (Miguélez-Rivera *et al.*, 2018) using an *in vitro* model of co-culture between rat NP/AF cells, macrophages and adipose-derived stem cells-conditioned medium showed a modulatory effect of the inflammatory response. A different pro-inflammatory/degenerative environment, as well as presence/absence of direct cell-cell communication seems to differently influence MSC and IVD cells response.

In the present study, it was observed a down-regulation of matrix degrading enzymes *bMMP-1*, *bMMP-3* and *bADAMTS-4* by AF cells in presence of MSC secretome.

Nonetheless, COL1 expression/production, as well as *bTIMP-1* and *bTIMP-2* expression were also decreased. Moreover, especially the secretome contributed to a weakening of the AF tissue. *In vivo* studies have shown a contribution of MSC transplantation to an upregulation of NP matrix protein COL2 with greater focus on the NP as reviewed by Sakai and Anderson (Sakai and Andersson, 2015); however, it has not been elucidated if this is due to the MSC differentiation into NP cells or to the stimulation of native NP cells to produce matrix proteins. The tissue regenerative potential of MSC secretome has been previously addressed in *in vivo* models of arthritis (Chen *et al.*, 2019; Kay *et al.*, 2017). One study showed that MSC secretome treatment suppressed the immune response and reduced cartilage damage by reducing aggrecan cleavage in arthritic mouse cartilage (Kay *et al.*, 2017). Another study in a rat model of induced osteoarthritis showed a higher cartilage content and a decreased ratio of MMP-13 to TIMP-1 after MSC secretome treatment (Chen *et al.*, 2019). Moreover, MSC-derived exosomes have also been shown to increase COL2 and aggrecan and decreased MMP-13 expression by chondrocytes isolated from a murine osteoarthritis model (Liu *et al.*, 2018), and to promote proliferation of NP cells and upregulation of aggrecan and COL2 (Lu *et al.*, 2017).

The limitations of this study include the proinflammatory degenerative microenvironment of the disc that cannot be completely simulated and the short investigation time in which the simulation of a therapy in a long-term perspective is not possible. Also, the communication between MSC and cells of the immune system cannot be simulated using this model. Moreover, the tensile strain applied to the system might have contributed to reduced MSC adhesion to the AF rings with time in culture and, therefore, explain that almost no effects were found in the co-culture group.

Overall, MSC immunomodulatory properties on the degenerative AF-OCs seemed to be mediated by a paracrine mechanism, indicating that the secretome has a potent modulatory effect on AF matrix turnover and inflammation. The present study confirmed the immunomodulatory and anti-catabolic effect of the MSC secretome in AF tissues in presence of a pro-inflammatory stimulus and supraphysiological loading, but it also seemed to contribute to a decrease in COL1 content and strength of the AF tissue. These results demonstrate that while MSC secretome-based treatment might be beneficial in the modulation of the inflammatory response of the IVD cells, they seem to contribute to further disc degeneration.

Conclusions

AF cells presented a proinflammatory/degenerative phenotype after CTS+IL-1β stimulation for 4 days. But, the previously described matrix weakening effect of the CTS+IL-1β stimulation did not correlate with changes in glycosaminoglycan, elastin or collagen tissue content. Interestingly, the MSC secretome contributed to a further decrease of collagen at gene/protein level, but with no changes in the AF mechanical strength. It also seemed to decrease the inflammatory and catabolic status of AF cells

activated by CTS+IL-1β, and to play a role in the regulation of the complement system and neovascularization. Ongoing studies with extended culture period are necessary to evaluate long-term changes in the AF matrix at protein level and alterations of mechanical properties.

Acknowledgements

The study was supported by the Ulm University (L.SBN.0157), German Research Foundation (NE_549/6-1), German Spine Society and German Academic Exchange Service. Andreas Ekkerlein received a dissertation scholarship by the Ulm University, and Raquel M. Goncalves was supported by the Alexander von Humboldt Foundation and by *Conselho de Reitores das Universidades Portuguesas*.

References

Adams MA, Roughley PJ (2006) What is intervertebral disc degeneration, and what causes it? Spine (Phila Pa 1976) **31**: 2151-2161.

Bendtsen M, Bunger C, Colombier P, Le Visage C, Roberts S, Sakai D, Urban JP (2016) Biological challenges for regeneration of the degenerated disc using cellular therapies. Acta Orthop **87**: 39-46.

Brisby H, Papadimitriou N, Brantsing C, Bergh P, Lindahl A, Barreto Henriksson H (2013) The presence of local mesenchymal progenitor cells in human degenerated intervertebral discs and possibilities to influence these in vitro: a descriptive study in humans. Stem Cells Dev **22**: 804-814.

Bustin SA, Benes V, Garson JA, Hellemans J, Huggett J, Kubista M, Mueller R, Nolan T, Pfaffl MW, Shipley GL, Vandesompele J, Wittwer CT (2009) The MIQE guidelines: minimum information for publication of quantitative real-time PCR experiments. Clin Chem **55**: 611-622.

Carrero R, Cerrada I, Lledó E, Dopazo J, García-García F, Rubio MP, Trigueros C, Dorronsoro A, Ruiz-Sauri A, Montero JA, Sepúlveda P (2012) IL1β induces mesenchymal stem cells migration and leucocyte chemotaxis through NF-κB. Stem Cell Rev Rep **8**: 905-916.

Chen W, Sun Y, Gu X, Hao Y, Liu X, Lin J, Chen J, Chen S (2019) Conditioned medium of mesenchymal stem cells delays osteoarthritis progression in a rat model by protecting subchondral bone, maintaining matrix homeostasis, and enhancing autophagy. J Tissue Eng Regen Med **13**: 1618-1628.

Cheng X, Zhang G, Zhang L, Hu Y, Zhang K, Sun X, Zhao C, Li H, Li YM, Zhao J (2018) Mesenchymal stem cells deliver exogenous miR-21 via exosomes to inhibit nucleus pulposus cell apoptosis and reduce intervertebral disc degeneration. J Cell Mol Med **22**: 261-276.

Cunha C, Almeida CR, Almeida MI, Silva AM, Molinos M, Lamas S, Pereira CL, Teixeira GQ, Monteiro AT, Santos SG, Gonçalves RM, Barbosa MA (2017) Systemic

delivery of bone marrow mesenchymal stem cells for in situ intervertebral disc regeneration. Stem Cells Transl Med **6**: 1029-1039.

Dai W, Hale SL, Kloner RA (2007) Role of a paracrine action of mesenchymal stem cells in the improvement of left ventricular function after coronary artery occlusion in rats. Regen Med **2**: 63-68.

Fan H, Zhao G, Liu L, Liu F, Gong W, Liu X, Yang L, Wang J, Hou Y (2012) Pre-treatment with IL-1β enhances the efficacy of MSC transplantation in DSS-induced colitis. Cell Mol Immunol **9**: 473-481.

Ferreira JR, Teixeira GQ, Santos SG, Barbosa MA, Almeida-Porada G, Goncalves RM (2018) Mesenchymal stromal cell secretome: influencing therapeutic potential by cellular pre-conditioning. Front Immunol **9**: 2837.

Gawri R, Rosenzweig DH, Krock E, Ouellet JA, Stone LS, Quinn TM, Haglund L (2014) High mechanical strain of primary intervertebral disc cells promotes secretion of inflammatory factors associated with disc degeneration and pain. Arthritis Res Ther **16**: R21.

Gilbert HT, Hoyland JA, Millward-Sadler SJ (2010) The response of human anulus fibrosus cells to cyclic tensile strain is frequency-dependent and altered with disc degeneration. Arthritis Rheum **62**: 3385-3394.

Gregory DE, Bae WC, Sah RL, Masuda K (2012) Anular delamination strength of human lumbar intervertebral disc. Eur Spine J **21**: 1716-1723.

Grönblad M, Habtemariam A, Virri J, Seitsalo S, Vanharanta H, Guyer RD (2003) Complement membrane attack complexes in pathologic disc tissues. Spine (Phila Pa 1976) **28**: 114-118.

Heuer F, Schmidt H, Wilke H-J (2008) The relation between intervertebral disc bulging and annular fiber associated strains for simple and complex loading. J Biomech **41**: 1086-1094.

Hyc A, Osiecka-Iwan A, Strzelczyk P, Moskalewski S (2003) Effect of IL-1beta, TNF-alpha and IL-4 on complement regulatory protein mRNA expression in human articular chondrocytes. Int J Mol Med **11**: 91-94.

Ignatius A, Schoengraf P, Kreja L, Liedert A, Recknagel S, Kandert S, Brenner RE, Schneider M, Lambris JD, Huber-Lang M (2011) Complement C3a and C5a modulate osteoclast formation and inflammatory response of osteoblasts in synergism with IL-1β. J Cell Biochem **112**: 2594-2605.

Kay AG, Long G, Tyler G, Stefan A, Broadfoot SJ, Piccinini AM, Middleton J, Kehoe O (2017) Mesenchymal Stem Cell-Conditioned Medium Reduces Disease Severity and Immune Responses in Inflammatory Arthritis. Sci Rep **7**: 18019.

Kohyama K, Saura R, Doita M, Mizuno K (2000) Intervertebral disc cell apoptosis by nitric oxide: biological understanding of intervertebral disc degeneration. Kobe J Med Sci **46**: 283-295.

Krampera M, Cosmi L, Angeli R, Pasini A, Liotta F, Andreini A, Santarlasci V, Mazzinghi B, Pizzolo G, Vinante F, Romagnani P, Maggi E, Romagnani S, Annunziato F (2006) Role for interferon-gamma in the immunomodulatory activity of human bone marrow mesenchymal stem cells. Stem Cells **24**: 386-398.

Liu Y, Lin L, Zou R, Wen C, Wang Z, Lin F (2018) MSC-derived exosomes promote proliferation and inhibit apoptosis of chondrocytes via lncRNA-KLF3-AS1/miR-206/GIT1 axis in osteoarthritis. Cell Cycle **17**: 2411-2422.

Lu K, Li HY, Yang K, Wu JL, Cai XW, Zhou Y, Li CQ (2017) Exosomes as potential alternatives to stem cell therapy for intervertebral disc degeneration: in-vitro study on exosomes in interaction of nucleus pulposus cells and bone marrow mesenchymal stem cells. Stem Cell Res Ther **8**: 108.

Melrose J, Smith SM, Appleyard RC, Little CB (2008) Aggrecan, versican and type VI collagen are components of annular translamellar crossbridges in the intervertebral disc. Eur Spine J **17**: 314-324.

Miguélez-Rivera L, Pérez-Castrillo S, González-Fernández ML, Prieto-Fernández JG, López-González ME, García-Cosamalón J, Villar-Suárez V (2018) Immunomodulation of mesenchymal stem cells in discogenic pain. Spine J **18**: 330-342.

Molinos M, Almeida CR, Caldeira J, Cunha C, Gonçalves RM, Barbosa MA (2015) Inflammation in intervertebral disc degeneration and regeneration. J R Soc Interface **12**: 20141191.

Moradi-Lakeh M, Forouzanfar MH, Vollset SE, El Bcheraoui C, Daoud F, Afshin A, Charara R, Khalil I, Higashi H, Abd El Razek MM, Kiadaliri AA, Alam K, Akseer N, Al-Hamad N, Ali R, AlMazroa MA, Alomari MA, Al-Rabeeah AA, Alsharif U, Altirkawi KA, Atique S, Badawi A, Barrero LH, Basulaiman M, Bazargan-Hejazi S, Bedi N, Bensenor IM, Buchbinder R, Danawi H, Dharmaratne SD, Zannad F, Farvid MS, Fereshtehnejad SM, Farzadfar F, Fischer F, Gupta R, Hamadeh RR, Hamidi S, Horino M, Hoy DG, Hsairi M, Husseini A, Javanbakht M, Jonas JB, Kasaeian A, Khan EA, Khubchandani J, Knudsen AK, Kopec JA, Lunevicius R, Abd El Razek HM, Majeed A, Malekzadeh R, Mate K, Mehari A, Meltzer M, Memish ZA, Mirarefin M, Mohammed S, Naheed A, Obermeyer CM, Oh IH, Park EK, Peprah EK, Pourmalek F, Qorbani M, Rafay A, Rahimi-Movaghar V, Shiri R, Rahman SU, Rai RK, Rana SM, Sepanlou SG, Shaikh MA, Shiue I, Sibai AM, Silva DAS, Singh JA, Skogen JC, Terkawi AS, Ukwaja KN, Westerman R, Yonemoto N, Yoon SJ, Younis MZ, Zaidi Z, Zaki MES, Lim SS, Wang H, Vos T, Naghavi M, Lopez AD, Murray CJL, Mokdad AH (2017) Burden of musculoskeletal disorders in the Eastern Mediterranean Region, 1990-2013: findings from the Global Burden of Disease Study 2013. Ann Rheum Dis **76**: 1365-1373.

Murray CJ, Barber RM, Foreman KJ, Abbasoglu Ozgoren A, Abd-Allah F, Abera SF, Aboyans V, Abraham JP, Abubakar I, Abu-Raddad LJ, Abu-Rmeileh NM, Achoki T, Ackerman IN, Ademi Z, Adou AK, Adsuar JC, Afshin A, Agardh EE, Alam SS, Alasfoor D, Albittar MI, Alegretti MA, Alemu ZA, Alfonso-Cristancho R, Alhabib S, Ali R, Alla F, Allebeck P, Almazroa MA, Alsharif U, Alvarez E, Alvis-Guzman N, Amare AT, Ameh EA, Amini H, Ammar W, Anderson HR, Anderson BO, Antonio CA, Anwari P, Arnlöv J, Arsic Arsenijevic VS, Artaman A, Asghar RJ, Assadi R, Atkins LS, Avila MA, Awuah B, Bachman VF, Badawi A, Bahit MC, Balakrishnan K, Banerjee A, Barker-Collo SL, Barquera S, Barregard L, Barrero LH, Basu A, Basu S, Basulaiman MO, Beardsley J, Bedi N, Beghi E, Bekele T, Bell ML, Benjet C, Bennett DA, Bensenor IM, Benzian H, Bernabé E, Bertozzi-Villa A, Beyene TJ, Bhala N, Bhalla A, Bhutta ZA,

Bienhoff K, Bikbov B, Biryukov S, Blore JD, Blosser CD, Blyth FM, Bohensky MA, Bolliger IW, Bora Başara B, Bornstein NM, Bose D, Boufous S, Bourne RR, Boyers LN, Brainin M, Brayne CE, Brazinova A, Breitborde NJ, Brenner H, Briggs AD, Brooks PM, Brown JC, Brugha TS, Buchbinder R, Buckle GC, Budke CM, Bulchis A, Bulloch AG, Campos-Nonato IR, Carabin H, Carapetis JR, Cárdenas R, Carpenter DO, Caso V, Castañeda-Orjuela CA, Castro RE, Catalá-López F, Cavalleri F, Çavlin A, Chadha VK, Chang JC, Charlson FJ, Chen H, Chen W, Chiang PP, Chimed-Ochir O, Chowdhury R, Christensen H, Christophi CA, Cirillo M, Coates MM, Coffeng LE, Coggeshall MS, Colistro V, Colquhoun SM, Cooke GS, Cooper C, Cooper LT, Coppola LM, Cortinovis M, Criqui MH, Crump JA, Cuevas-Nasu L, Danawi H, Dandona L, Dandona R, Dansereau E, Dargan PI, Davey G, Davis A, Davitoiu DV, Dayama A, De Leo D, Degenhardt L, Del Pozo-Cruz B, Dellavalle RP, Deribe K, Derrett S, Des Jarlais DC, Dessalegn M, Dharmaratne SD, Dherani MK, Diaz-Torné C, Dicker D, Ding EL, Dokova K, Dorsey ER, Driscoll TR, Duan L, Duber HC, Ebel BE, Edmond KM, Elshrek YM, Endres M, Ermakov SP, Erskine HE, Eshrati B, Esteghamati A, Estep K, Faraon EJ, Farzadfar F, Fay DF, Feigin VL, Felson DT, Fereshtehnejad SM, Fernandes JG, Ferrari AJ, Fitzmaurice C, Flaxman AD, Fleming TD, Foigt N, Forouzanfar MH, Fowkes FG, Paleo UF, Franklin RC, Fürst T, Gabbe B, Gaffikin L, Gankpé FG, Geleijnse JM, Gessner BD, Gething P, Gibney KB, Giroud M, Giussani G, Gomez Dantes H, Gona P, González-Medina D, Gosselin RA, Gotay CC, Goto A, Gouda HN, Graetz N, Gugnani HC, Gupta R, Gupta R, Gutiérrez RA, Haagsma J, Hafezi-Nejad N, Hagan H, Halasa YA, Hamadeh RR, Hamavid H, Hammami M, Hancock J, Hankey GJ, Hansen GM, Hao Y, Harb HL, Haro JM, Havmoeller R, Hay SI, Hay RJ, Heredia-Pi IB, Heuton KR, Heydarpour P, Higashi H, Hijar M, Hoek HW, Hoffman HJ, Hosgood HD, Hossain M, Hotez PJ, Hoy DG, Hsairi M, Hu G, Huang C, Huang JJ, Husseini A, Huynh C, Iannarone ML, Iburg KM, Innos K, Inoue M, Islami F, Jacobsen KH, Jarvis DL, Jassal SK, Jee SH, Jeemon P, Jensen PN, Jha V, Jiang G, Jiang Y, Jonas JB, Juel K, Kan H, Karch A, Karema CK, Karimkhani C, Karthikeyan G, Kassebaum NJ, Kaul A, Kawakami N, Kazanjan K, Kemp AH, Kengne AP, Keren A, Khader YS, Khalifa SE, Khan EA, Khan G, Khang YH, Kieling C, Kim D, Kim S, Kim Y, Kinfu Y, Kinge JM, Kivipelto M, Knibbs LD, Knudsen AK, Kokubo Y, Kosen S, Krishnaswami S, Kuate Defo B, Kucuk Bicer B, Kuipers EJ, Kulkarni C, Kulkarni VS, Kumar GA, Kyu HH, Lai T, Lalloo R, Lallukka T, Lam H, Lan Q, Lansingh VC, Larsson A, Lawrynowicz AE, Leasher JL, Leigh J, Leung R, Levitz CE, Li B, Li Y, Li Y, Lim SS, Lind M, Lipshultz SE, Liu S, Liu Y, Lloyd BK, Lofgren KT, Logroscino G, Looker KJ, Lortet-Tieulent J, Lotufo PA, Lozano R, Lucas RM, Lunevicius R, Lyons RA, Ma S, Macintyre MF, Mackay MT, Majdan M, Malekzadeh R, Marcenes W, Margolis DJ, Margono C, Marzan MB, Masci JR, Mashal MT, Matzopoulos R, Mayosi BM, Mazorodze TT, McGill NW, McGrath JJ, McKee M, McLain A, Meaney PA, Medina C, Mehndiratta MM, Mekonnen W, Melaku YA, Meltzer M, Memish ZA, Mensah GA, Meretoja A, Mhimbira FA, Micha R, Miller TR, Mills EJ, Mitchell PB, Mock CN, Mohamed Ibrahim N, Mohammad KA, Mokdad AH, Mola GL, Monasta L, Montañez Hernandez JC, Montico M, Montine TJ, Mooney MD, Moore AR, Moradi-Lakeh M, Moran AE, Mori R, Moschandreas J, Moturi WN,

Moyer ML, Mozaffarian D, Msemburi WT, Mueller UO, Mukaigawara M, Mullany EC, Murdoch ME, Murray J, Murthy KS, Naghavi M, Naheed A, Naidoo KS, Naldi L, Nand D, Nangia V, Narayan KM, Nejjari C, Neupane SP, Newton CR, Ng M, Ngalesoni FN, Nguyen G, Nisar MI, Nolte S, Norheim OF, Norman RE, Norrving B, Nyakarahuka L, Oh IH, Ohkubo T, Ohno SL, Olusanya BO, Opio JN, Ortblad K, Ortiz A, Pain AW, Pandian JD, Panelo CI, Papachristou C, Park EK, Park JH, Patten SB, Patton GC, Paul VK, Pavlin BI, Pearce N, Pereira DM, Perez-Padilla R, Perez-Ruiz F, Perico N, Pervaiz A, Pesudovs K, Peterson CB, Petzold M, Phillips MR, Phillips BK, Phillips DE, Piel FB, Plass D, Poenaru D, Polinder S, Pope D, Popova S, Poulton RG, Pourmalek F, Prabhakaran D, Prasad NM, Pullan RL, Qato DM, Quistberg DA, Rafay A, Rahimi K, Rahman SU, Raju M, Rana SM, Razavi H, Reddy KS, Refaat A, Remuzzi G, Resnikoff S, Ribeiro AL, Richardson L, Richardus JH, Roberts DA, Rojas-Rueda D, Ronfani L, Roth GA, Rothenbacher D, Rothstein DH, Rowley JT, Roy N, Ruhago GM, Saeedi MY, Saha S, Sahraian MA, Sampson UK, Sanabria JR, Sandar L, Santos IS, Satpathy M, Sawhney M, Scarborough P, Schneider IJ, Schöttker B, Schumacher AE, Schwebel DC, Scott JG, Seedat S, Sepanlou SG, Serina PT, Servan-Mori EE, Shackelford KA, Shaheen A, Shahraz S, Shamah Levy T, Shangguan S, She J, Sheikhbahaei S, Shi P, Shibuya K, Shinohara Y, Shiri R, Shishani K, Shiue I, Shrime MG, Sigfusdottir ID, Silberberg DH, Simard EP, Sindi S, Singh A, Singh JA, Singh L, Skirbekk V, Slepak EL, Sliwa K, Soneji S, Søreide K, Soshnikov S, Sposato LA, Sreeramareddy CT, Stanaway JD, Stathopoulou V, Stein DJ, Stein MB, Steiner C, Steiner TJ, Stevens A, Stewart A, Stovner LJ, Stroumpoulis K, Sunguya BF, Swaminathan S, Swaroop M, Sykes BL, Tabb KM, Takahashi K, Tandon N, Tanne D, Tanner M, Tavakkoli M, Taylor HR, Te Ao BJ, Tediosi F, Temesgen AM, Templin T, Ten Have M, Tenkorang EY, Terkawi AS, Thomson B, Thorne-Lyman AL, Thrift AG, Thurston GD, Tillmann T, Tonelli M, Topouzis F, Toyoshima H, Traebert J, Tran BX, Trillini M, Truelsen T, Tsilimbaris M, Tuzcu EM, Uchendu US, Ukwaja KN, Undurraga EA, Uzun SB, Van Brakel WH, Van De Vijver S, van Gool CH, Van Os J, Vasankari TJ, Venketasubramanian N, Violante FS, Vlassov VV, Vollset SE, Wagner GR, Wagner J, Waller SG, Wan X, Wang H, Wang J, Wang L, Warouw TS, Weichenthal S, Weiderpass E, Weintraub RG, Wenzhi W, Werdecker A, Westerman R, Whiteford HA, Wilkinson JD, Williams TN, Wolfe CD, Wolock TM, Woolf AD, Wulf S, Wurtz B, Xu G, Yan LL, Yano Y, Ye P, Yentür GK, Yip P, Yonemoto N, Yoon SJ, Younis MZ, Yu C, Zaki ME, Zhao Y, Zheng Y, Zonies D, Zou X, Salomon JA, Lopez AD, Vos T (2015) Global, regional, and national disability-adjusted life years (DALYs) for 306 diseases and injuries and healthy life expectancy (HALE) for 188 countries, 1990-2013: quantifying the epidemiological transition. Lancet **386**: 2145-2191.

Naqvi SM, Buckley CT (2015) Extracellular matrix production by nucleus pulposus and bone marrow stem cells in response to altered oxygen and glucose microenvironments. J Anat **227**: 757-766.

Naqvi SM, Buckley CT (2016) Bone marrow stem cells in response to intervertebral disc-like matrix acidity and oxygen concentration: implications for cell-based regenerative therapy. Spine (Phila Pa 1976) **41**: 743-750.

Neidlinger-Wilke C, Mietsch A, Rinkler C, Wilke HJ, Ignatius A, Urban J (2012) Interactions of environmental conditions and mechanical loads have influence on matrix turnover by nucleus pulposus cells. J Orthop Res **30**: 112-121.

Noriega DC, Ardura F, Hernández-Ramajo R, Martín-Ferrero M, Sánchez-Lite I, Toribio B, Alberca M, García V, Moraleda JM, Sánchez A, García-Sancho J (2017) Intervertebral disc repair by allogeneic mesenchymal bone marrow cells: a randomized controlled trial. Transplantation **101**: 1945-1951.

Noris M, Remuzzi G (2013) Overview of complement activation and regulation. Semin Nephrol **33**: 479-492.

Orozco L, Soler R, Morera C, Alberca M, Sánchez A, García-Sancho J (2011) Intervertebral disc repair by autologous mesenchymal bone marrow cells: a pilot study. Transplantation **92**: 822-828.

Parekkadan B, van Poll D, Suganuma K, Carter EA, Berthiaume F, Tilles AW, Yarmush ML (2007) Mesenchymal stem cell-derived molecules reverse fulminant hepatic failure. PLoS One **2**: e941.

Pereira CL, Teixeira GQ, Ribeiro-Machado C, Caldeira J, Costa M, Figueiredo F, Fernandes R, Aguiar P, Grad S, Barbosa MA, Gonçalves RM (2016) Mesenchymal Stem/Stromal Cells seeded on cartilaginous endplates promote intervertebral disc regeneration through extracellular matrix remodeling. Sci Rep **6**: 33836.

Pettine K, Suzuki R, Sand T, Murphy M (2016) Treatment of discogenic back pain with autologous bone marrow concentrate injection with minimum two year follow-up. Int Orthop **40**: 135-140.

Pettine KA, Murphy MB, Suzuki RK, Sand TT (2015) Percutaneous injection of autologous bone marrow concentrate cells significantly reduces lumbar discogenic pain through 12 months. Stem Cells **33**: 146-156.

Pratsinis H, Papadopoulou A, Neidlinger-Wilke C, Brayda-Bruno M, Wilke HJ, Kletsas D (2016) Cyclic tensile stress of human annulus fibrosus cells induces MAPK activation: involvement in proinflammatory gene expression. Osteoarthritis Cartilage **24**: 679-687.

Ren G, Zhang L, Zhao X, Xu G, Zhang Y, Roberts AI, Zhao RC, Shi Y (2008) Mesenchymal stem cell-mediated immunosuppression occurs via concerted action of chemokines and nitric oxide. Cell Stem Cell **2**: 141-150.

Ricklin D, Lambris JD (2013) Complement in immune and inflammatory disorders: pathophysiological mechanisms. J Immunol **190**: 3831-3838.

Risbud MV, Shapiro IM (2014) Role of cytokines in intervertebral disc degeneration: pain and disc content. Nat Rev Rheumatol **10**: 44-56.

Roberts S, Evans H, Trivedi J, Menage J (2006) Histology and pathology of the human intervertebral disc. J Bone Joint Surg Am **88 Suppl 2**: 10-14.

Saggese T, Teixeira GQ, Wade K, Moll L, Ignatius A, Wilke HJ, Goncalves RM, Neidlinger-Wilke C (2019) GEORG SCHMORL PRIZE OF THE GERMAN SPINE SOCIETY (DWG) 2018: combined inflammatory and mechanical stress weakens the annulus fibrosus: evidences from a loaded bovine AF organ culture. Eur Spine J **28**: 922-933.

Sakai D, Andersson GB (2015) Stem cell therapy for intervertebral disc regeneration: obstacles and solutions. Nat Rev Rheumatol **11**: 243-256.

Sakai D, Grad S (2015) Advancing the cellular and molecular therapy for intervertebral disc disease. Adv Drug Deliv Rev **84**: 159-171.

Sakai D, Nakamura Y, Nakai T, Mishima T, Kato S, Grad S, Alini M, Risbud MV, Chan D, Cheah KS, Yamamura K, Masuda K, Okano H, Ando K, Mochida J (2012) Exhaustion of nucleus pulposus progenitor cells with ageing and degeneration of the intervertebral disc. Nat Commun **3**: 1264.

Saparov A, Ogay V, Nurgozhin T, Jumabay M, Chen WC (2016) Preconditioning of Human Mesenchymal Stem Cells to Enhance Their Regulation of the Immune Response. Stem Cells Int **2016**: 3924858.

Soland MA, Bego M, Colletti E, Zanjani ED, St. Jeor S, Porada CD, Almeida-Porada G (2013) Mesenchymal stem cells engineered to inhibit complement-mediated damage. PLoS One **8**: e60461.

Strassburg S, Richardson SM, Freemont AJ, Hoyland JA (2010) Co-culture induces mesenchymal stem cell differentiation and modulation of the degenerate human nucleus pulposus cell phenotype. Regen Med **5**: 701-711.

Teixeira GQ, Boldt A, Nagl I, Pereira CL, Benz K, Wilke HJ, Ignatius A, Barbosa MA, Goncalves RM, Neidlinger-Wilke C (2016) A degenerative/proinflammatory intervertebral disc organ culture: an ex vivo model for anti-inflammatory drug and cell therapy. Tissue Eng Part C Methods **22**: 8-19.

Teixeira GQ, Pereira CL, Ferreira JR, Maia AF, Gomez-Lazaro M, Barbosa MA, Neidlinger-Wilke C, Goncalves RM (2018) Immunomodulation of human mesenchymal stem/stromal cells in intervertebral disc degeneration: insights from a proinflammatory/degenerative ex vivo model. Spine (Phila Pa 1976) **43**: E673-E682.

Tu Z, Li Q, Bu H, Lin F (2010) Mesenchymal stem cells inhibit complement activation by secreting factor H. Stem Cells Dev **19**: 1803-1809.

Urban JP (2002) The role of the physicochemical environment in determining disc cell behaviour. Biochem Soc Trans **30**: 858-864.

van Buul GM, Villafuertes E, Bos PK, Waarsing JH, Kops N, Narcisi R, Weinans H, Verhaar JA, Bernsen MR, van Osch GJ (2012) Mesenchymal stem cells secrete factors that inhibit inflammatory processes in short-term osteoarthritic synovium and cartilage explant culture. Osteoarthritis Cartilage **20**: 1186-1196.

van Koppen A, Joles JA, van Balkom BW, Lim SK, de Kleijn D, Giles RH, Verhaar MC (2012) Human embryonic mesenchymal stem cell-derived conditioned medium rescues kidney function in rats with established chronic kidney disease. PLoS One **7**: e38746.

Vergroesen PP, Kingma I, Emanuel KS, Hoogendoorn RJ, Welting TJ, van Royen BJ, van Dieën JH, Smit TH (2015) Mechanics and biology in intervertebral disc degeneration: a vicious circle. Osteoarthritis Cartilage **23**: 1057-1070.

Wang Q, Rozelle AL, Lepus CM, Scanzello CR, Song JJ, Larsen DM, Crish JF, Bebek G, Ritter SY, Lindstrom TM, Hwang I, Wong HH, Punzi L, Encarnacion A, Shamloo M, Goodman SB, Wyss-Coray T, Goldring SR, Banda NK, Thurman JM,

Gobezie R, Crow MK, Holers VM, Lee DM, Robinson WH (2011) Identification of a central role for complement in osteoarthritis. Nat Med **17**: 1674-1679.

Wuertz K, Godburn K, Iatridis JC (2009) MSC response to pH levels found in degenerating intervertebral discs. Biochem Biophys Res Commun **379**: 824-829.

Yoshikawa T, Ueda Y, Miyazaki K, Koizumi M, Takakura Y (2010) Disc regeneration therapy using marrow mesenchymal cell transplantation: a report of two case studies. Spine (Phila Pa 1976) **35**: E475-480.

Yu J, Schollum ML, Wade KR, Broom ND, Urban JP (2015) ISSLS Prize Winner: a detailed examination of the elastic network leads to a new understanding of annulus fibrosus organization. Spine (Phila Pa 1976) **40**: 1149-1157.

Figure legends

Fig. 1. Experimental timeline and experimental groups. (**a**) MSC secretome was produced by 10^6 MSC preconditioned with 10 ng/mL IL-1β medium supplementation and culture at 37 °C with 6 % O_2 and 8.5 % CO_2 for 48 h (5 mL/well in 6-well culture plates). (**b**) The annulus fibrosus (AF) rings were cultured in a custom-made electromechanical device for the application of cyclic tensile strain (CTS) to deformable silicone dishes and with IL-1β in the culture medium. The stimulated AF-OCs were either treated with MSC in co-culture or MSC secretome.

Fig. 2. Cell viability and gene expression of bovine AF cells at day 11 of organ culture. (**a**) Mitochondrial metabolic activity of AF organ cultures expressed in relative fluorescence units normalized to tissue wet weight. (**b**) Relative mRNA expression of bovine cell survival marker *bNOS2*, (**c**) pro-inflammatory markers, and (**d**) complement regulators. Results were normalised to expression level of *bGAPDH*. n = 5-12, * $p < 0.05$, ** $p < 0.01$, *** $p < 0.001$.

Fig. 3. Gene expression of bovine AF cells at day 11 of organ culture. (**a**) Relative mRNA expression of bovine matrix components, (**b**) tissue inhibitors of metalloproteinases, (**c**) matrix degrading enzymes, and (**d**) vascularization marker *bVEGF*. Results were normalised to expression level of *bGAPDH*. n = 6-12, * $p < 0.05$, ** $p < 0.01$, *** $p < 0.001$.

Fig. 4. DNA and protein content of AF-OCs at day 11. (**a**) DNA amount (ng) released to the culture supernatants. (**b**) DNA content in the AF tissues normalized to wet weight (ng/mg). (**c**) Collagen, elastin and sulphated glycosaminoglycan (sGAG) content in the AF tissues normalized to wet weight (μg/mg). n = 10-18, * $p < 0.05$, **** $p < 0.0001$.

Fig. 5. IL-6 and MMP-3 content of AF-OCs at day 11. (**a**) Representative images under polarized-light and bright-field of IL-6 and MMP-3 distribution within the translamellar bridging network (TLBN, *yellow arrows*) and the lamella matrix (LM, *green arrows*) of AF-OCs; *scale bar*, 500 μm. (**b**) IL-6 and (**c**) MMP-3 staining intensity in the TLBM normalized to the LM and to the unstimulated control sample for each experiment. n = 7-10; ## $p < 0.01$ (significant effect of control, *dashed line*); * $p < 0.05$, ** $p < 0.01$ (significant effects between CTS+IL-1β stimulation and treatments).

Fig. 6. Protein content of AF-OC supernatants at day 11. (**a**) PGE_2 (ng/mL), (**b**) bovine IL-6 (bIL-6, pg/mL), (**c**) human IL-6 (hIL-6, ng/mL), (**d**) hCFH (ng/mL), and (**e**) hTIMP-1 and hTIMP-2 concentration (ng/mL). n = 6-12, * $p < 0.05$, *** $p < 0.001$, **** $p < 0.0001$.

Fig. 7. Cell viability and protein content of AF-OC supernatants at day 16. (**a**) Mitochondrial metabolic activity of AF organ cultures expressed in relative

fluorescence units normalized to tissue wet weight. (**b**) PGE_2 (ng/mL), (**c**) bovine IL-6 (bIL-6, pg/mL), (**d**) human IL-6 (hIL-6, ng/mL), (**e**) hCFH (ng/mL), and (**f**) hTIMP-2 concentration (ng/mL). n = 6-8, * $p < 0.05$, ** $p < 0.01$.

Fig. 8. Annular delamination strength of AF-OCs at day 16. Peel strength as function of displacement rate (N/mm). n = 6-12, * $p < 0.05$.

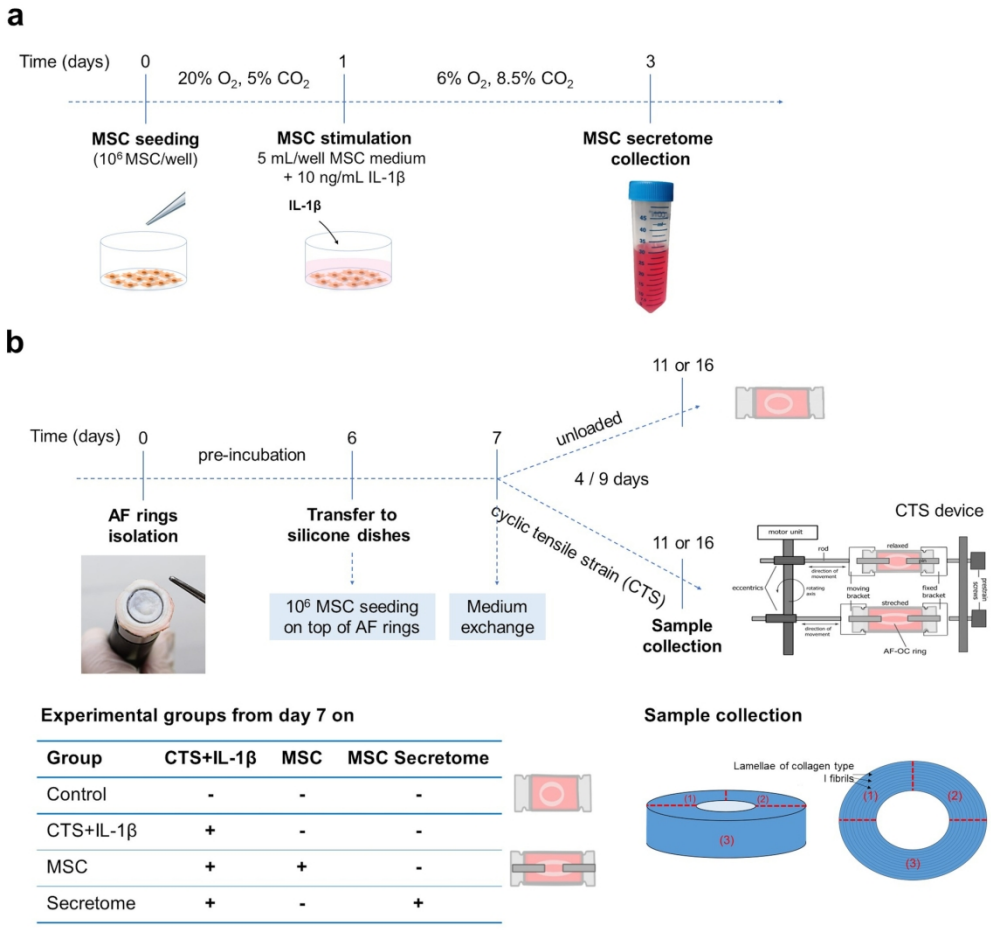

Fig. 1. Experimental timeline and experimental groups. (**a**) MSC secretome was produced by 10^6 MSC preconditioned with 10 ng/mL IL-1β medium supplementation and culture at 37 °C with 6 % O_2 and 8.5 % CO_2 for 48 h (5 mL/well in 6-well culture plates). (**b**) The annulus fibrosus (AF) rings were cultured in a custom-made electromechanical device for the application of cyclic tensile strain (CTS) to deformable silicone dishes and with IL-1β in the culture medium. The stimulated AF-OCs were either treated with MSC in co-culture or MSC secretome.

170x159mm (300 x 300 DPI)

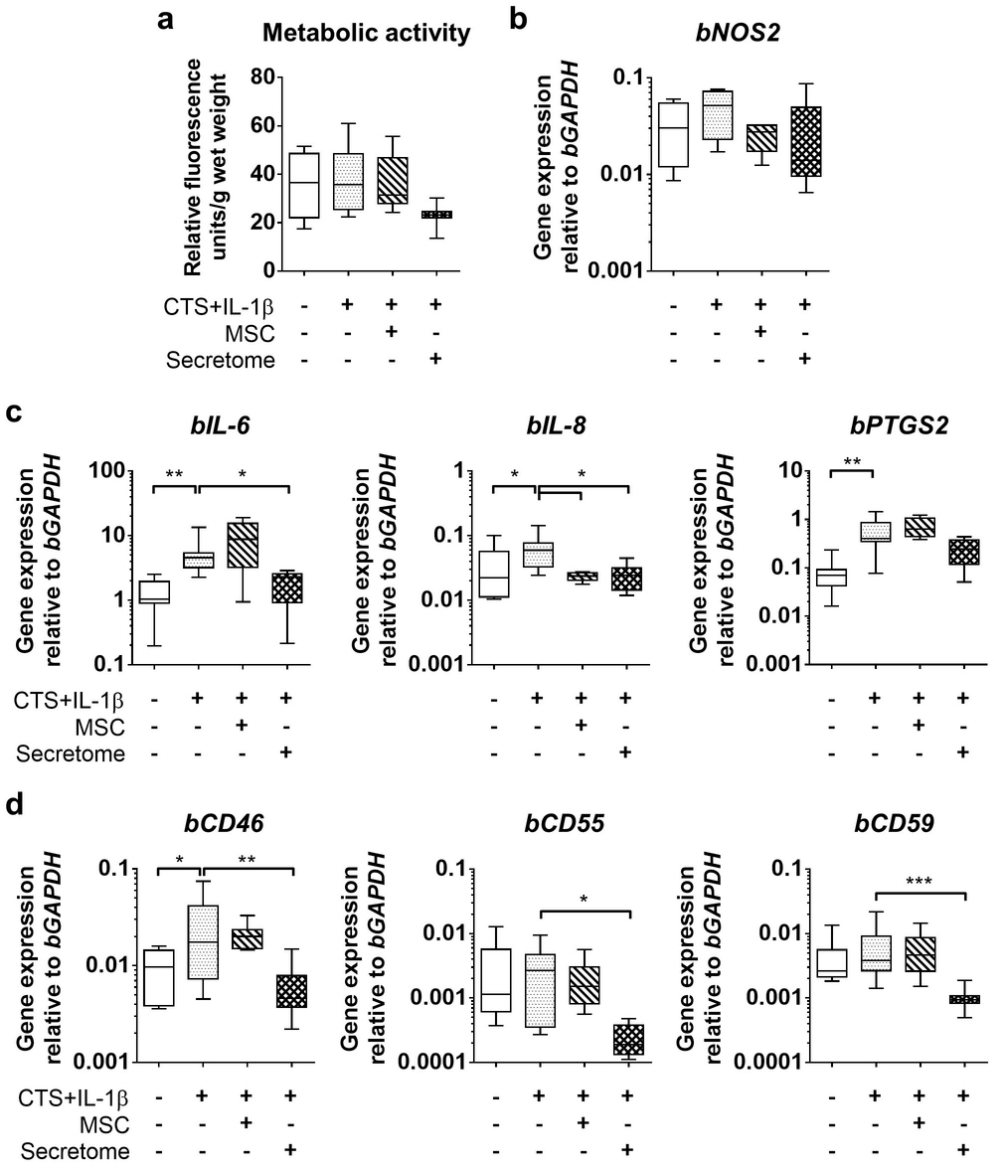

Fig. 2. Cell viability and gene expression of bovine AF cells at day 11 of organ culture. (**a**) Mitochondrial metabolic activity of AF organ cultures expressed in relative fluorescence units normalized to tissue wet weight. (**b**) Relative mRNA expression of bovine cell survival marker *bNOS2*, (**c**) pro-inflammatory markers, and (**d**) complement regulators. Results were normalised to expression level of *bGAPDH*. n = 5-12, * $p < 0.05$, ** $p < 0.01$, *** $p < 0.001$.

85x100mm (300 x 300 DPI)

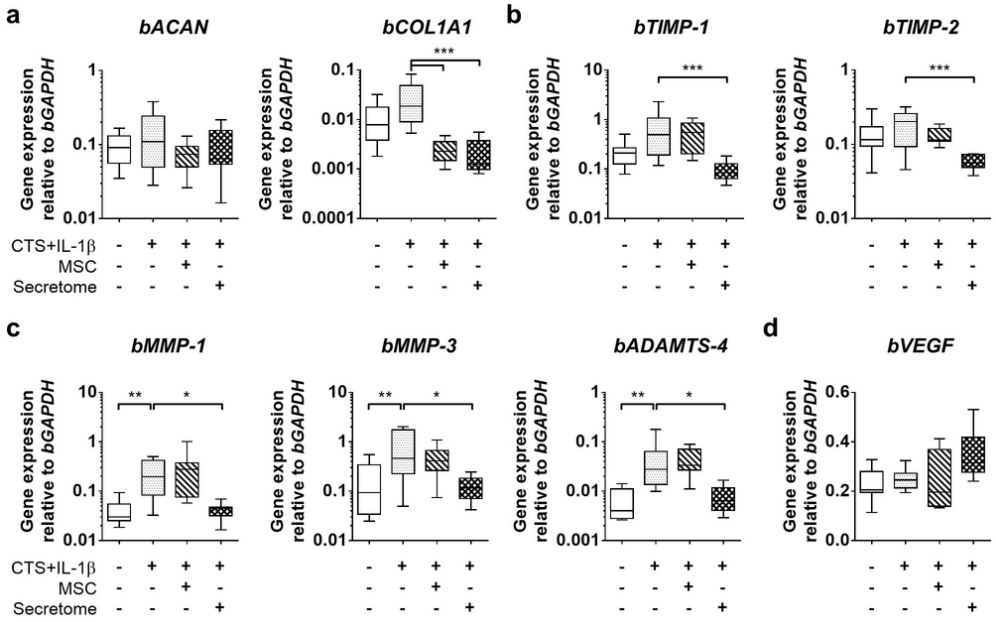

Fig. 3. Gene expression of bovine AF cells at day 11 of organ culture. (**a**) Relative mRNA expression of bovine matrix components, (**b**) tissue inhibitors of metalloproteinases, (**c**) matrix degrading enzymes, and (**d**) vascularization marker *bVEGF*. Results were normalised to expression level of *bGAPDH*. n = 6-12, * $p < 0.05$, ** $p < 0.01$, *** $p < 0.001$.

85x54mm (300 x 300 DPI)

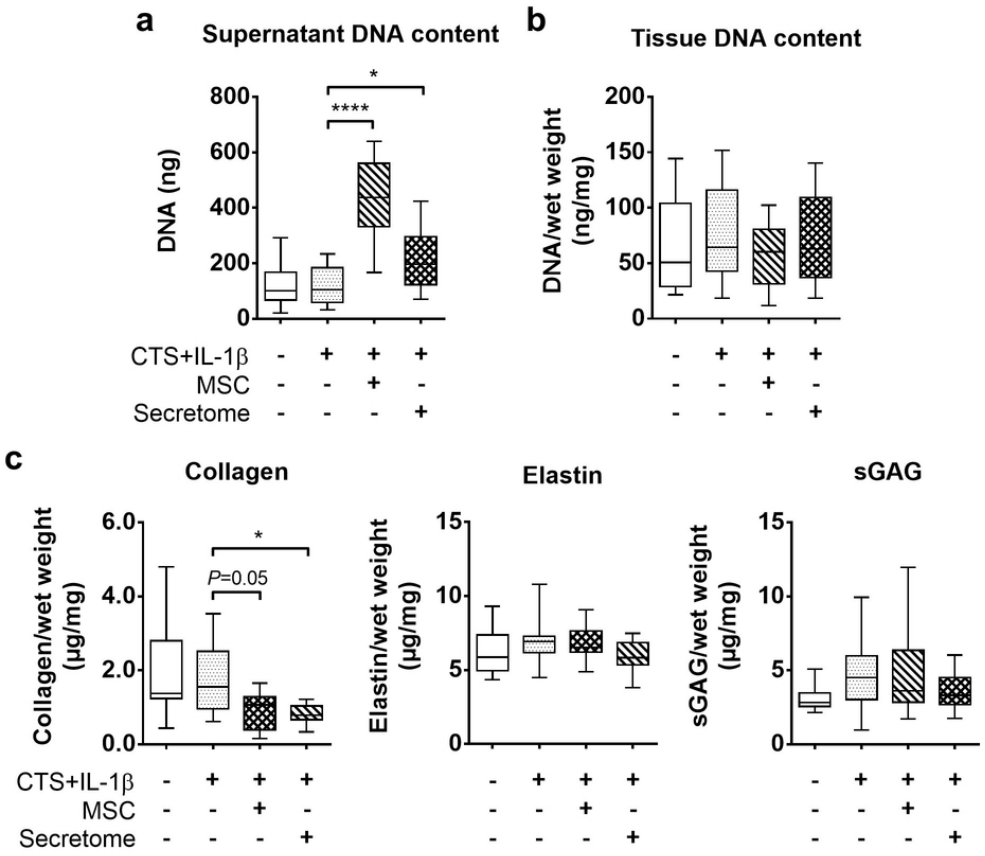

Fig. 4. DNA and protein content of AF-OCs at day 11. (**a**) DNA amount (ng) released to the culture supernatants. (**b**) DNA content in the AF tissues normalized to wet weight (ng/mg). (**c**) Collagen, elastin and sulphated glycosaminoglycan (sGAG) content in the AF tissues normalized to wet weight (μg/mg). n = 10-18, * $p < 0.05$, **** $p < 0.0001$.

79x69mm (300 x 300 DPI)

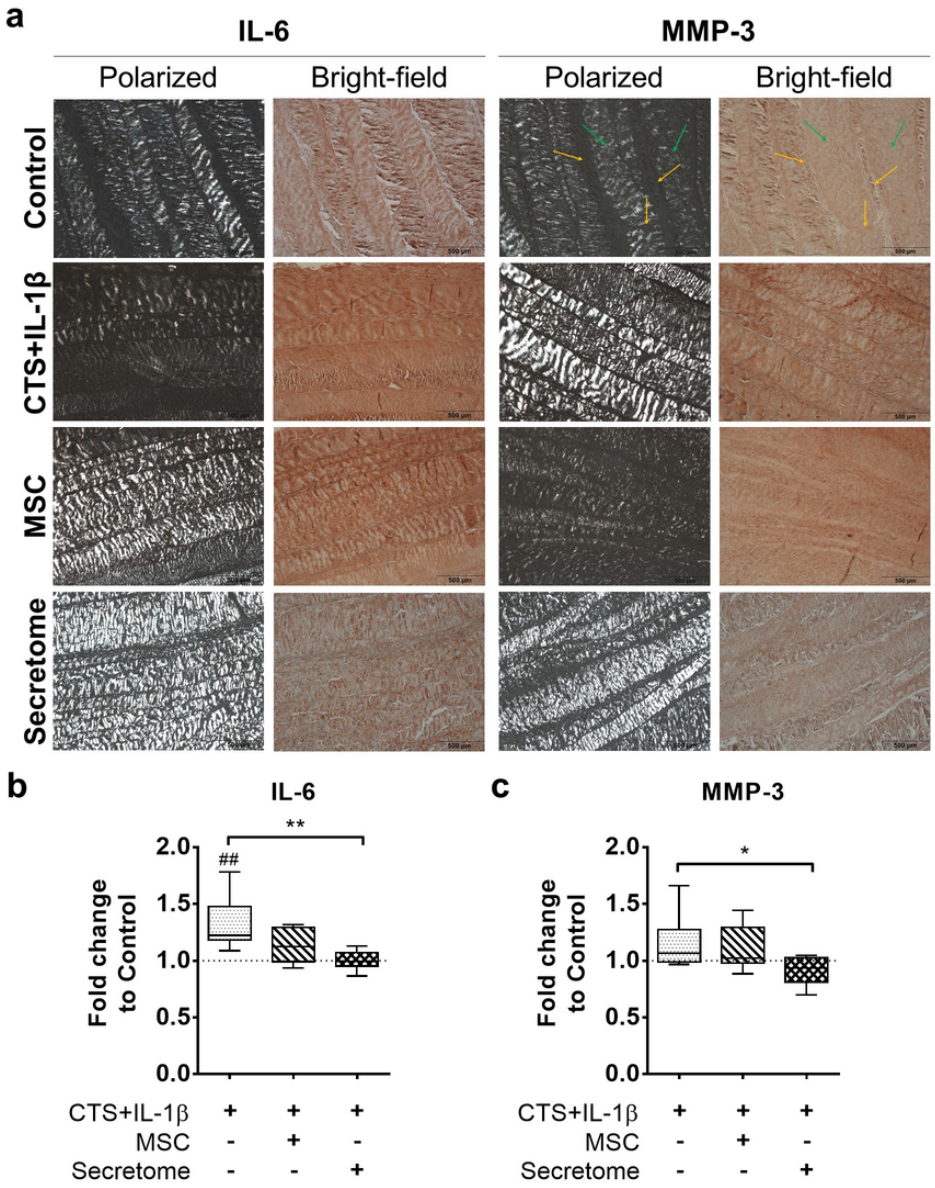

Fig. 5. IL-6 and MMP-3 content of AF-OCs at day 11. (**a**) Representative images under polarized-light and bright-field of IL-6 and MMP-3 distribution within the translamellar bridging network (TLBN, *yellow arrows*) and the lamella matrix (LM, *green arrows*) of AF-OCs; scale bar, 500 µm. (**b**) IL-6 and (**c**) MMP-3 staining intensity in the TLBM normalized to the LM and to the unstimulated control sample for each experiment. n = 7-10; ## $p < 0.01$ (significant effect compared to control, *dashed line*); * $p < 0.05$, ** $p < 0.01$ (significant effects between CTS+IL-1β stimulation and treatments).

72x92mm (300 x 300 DPI)

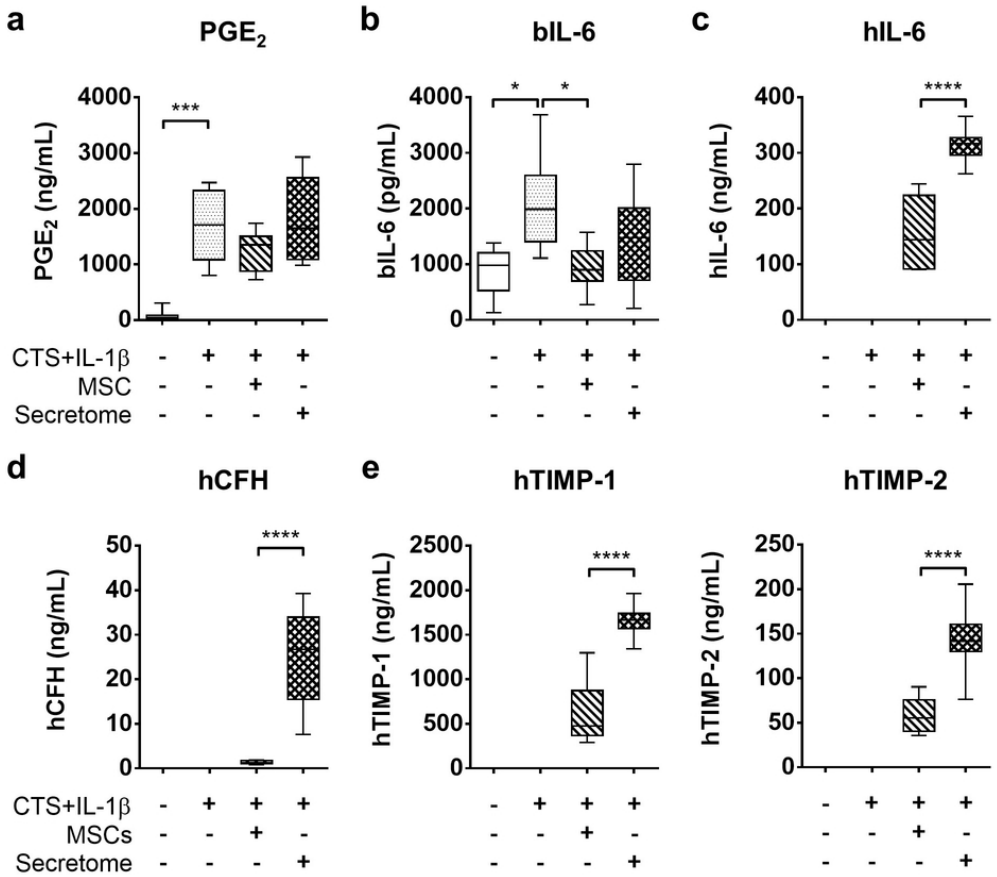

Fig. 6. Protein content of AF-OC supernatants at day 11. (**a**) PGE_2 (ng/mL), (**b**) bovine IL-6 (bIL-6, pg/mL), (**c**) human IL-6 (hIL-6, ng/mL), (**d**) hCFH (ng/mL), and (**e**) hTIMP-1 and hTIMP-2 concentration (ng/mL). n = 6-12, * $p < 0.05$, *** $p < 0.001$, **** $p < 0.0001$.

79x70mm (300 x 300 DPI)

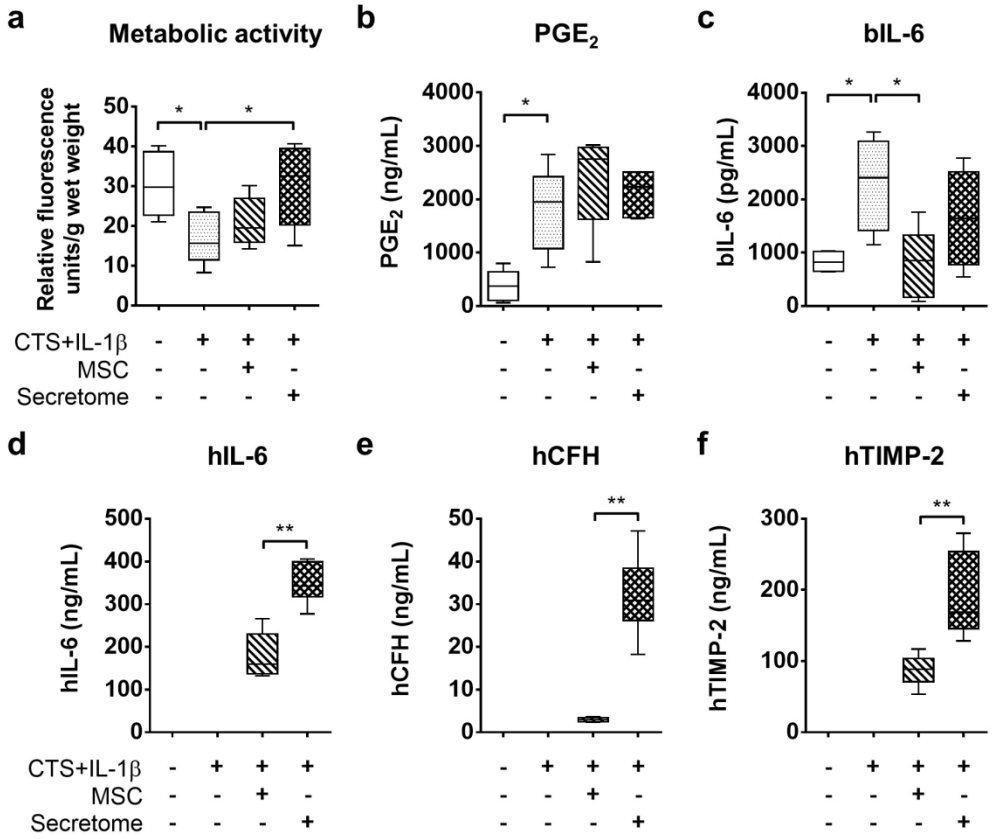

Fig. 7. Cell viability and protein content of AF-OC supernatants at day 16. (**a**) Mitochondrial metabolic activity of AF organ cultures expressed in relative fluorescence units normalized to tissue wet weight. (**b**) PGE_2 (ng/mL), (**c**) bovine IL-6 (bIL-6, pg/mL), (**d**) human IL-6 (hIL-6, ng/mL), (**e**) hCFH (ng/mL), and (**f**) hTIMP-2 concentration (ng/mL). n = 6-8, * $p < 0.05$, ** $p < 0.01$.

518x444mm (96 x 96 DPI)

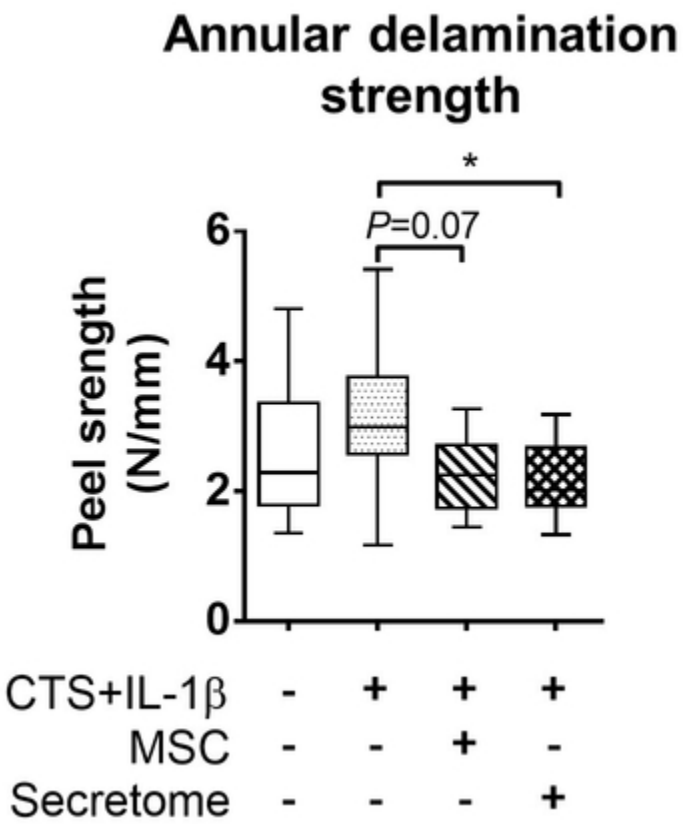

Fig. 8. Annular delamination strength of AF-OCs at day 16. Peel strength as function of displacement rate (N/mm). n = 6-12, * $p < 0.05$.

32x35mm (300 x 300 DPI)

Table 1. Media added at days 7 and 11 of culture to the different experimental groups. CTS: cyclic tensile strain; IL-1β: interleukin-1β; IVD: intervertebral disc; MSC: mesenchymal stem cells

Group	Medium
Control	IVD medium
CTS+IL-1β	IVD medium + 10 ng/mL IL-1β
MSC	IVD medium + 10 ng/mL IL-1β
Secretome	IVD medium + MSC Secretome (1:1 ratio) + 10 ng/mL IL-1β

Table 2. Bovine oligonucleotide primers used for qRT-PCR. Primers with shown sequence were custom designed; primers with assay ID number were purchased from Applied Biosystems. fw: forward; rev: reverse; b: bovine.

Gene	Sequence (forward and reverse primer)	Product size (bp)
bACAN	fw: 5′-ACA GCG CCT ACC AAG ACA AG-3′ rev: 5′-ACG ATG CCT TTT ACC ACG AC- 3′	155
bADAMTS-4	fw: 5′-GAA GCA ATG CAC TGG TCT GA-3′ rev: 5′-CTA GGA GAC AGT GCC CGA AG-3′	155
bCD46	assay ID: Bt03224806_m1	97
bCD55	assay ID: Bt03220649_m1	67
bCD59	assay ID: Bt03229098_m1	135
bCOL1A1	assay ID: Bt01463861_g1	61
bGAPDH	fw: 5′-ACC CAG AAG ACT GTG GAT GG-3′ rev: 5′-CAA CAG ACA CGT TGG GAG TG-3′	178
bIL-6	fw: 5′-ACC CCA GGC AGA CTA CTT CT-3′ rev: 5′-GCA TCC GTC CTT TTC CTC CA-3′	183
bIL-8	fw: 5′-ATT CCA CAC CTT TCC ACC CC-3′ rev: 5′-ACA ACC TTC TGC ACC CAC TT-3′	148
bMMP-1	fw: 5′-ATG CTG TTT TCC AGA AAG GTG G-3′ rev: 5′-TCA GGA AAC ACC TTC CAC AGA C-3′	193
bMMP-3	assay ID: Bt04259490_m1	76
bNOS2	assay ID: Bt03249602_g1	56
bPTGS2	assay ID: Bt03214492_m1	87
bTIMP-1	assay ID: Bt03223721_m1	57
bTIMP-2	assay ID: Bt03231007_m1	88
bVEGF	fw: 5′-TTG CCT TGC TGC TCT ACC TT-3′ rev: 5′-ACA CAG GAC GGC TTG AAA AT-3′	196

Supplemental Data

To evaluate whether the proinflammatory/degenerative conditions of the annulus fibrosus organ culture (AF-OC) could influence the mesenchymal stem/stromal cells (MSC) phenotype, the gene expression of several markers by the MSC was analysed after expansion (Basal MSC) and after preconditioning with 10 ng/mL IL-1β medium supplementation and culture at 37 °C with 6 % O2 and 8.5 % CO2 for 48 h (pre-conditioned MSC).

Materials and Methods

Gene expression analysis of human MSC

Total RNA was isolated from the MSC using the RNeasy Mini kit (Qiagen). RNA concentration and quality were determined by spectrophotometry (Spark, Tecan). For cDNA synthesis, 1 µg of RNA was reverse transcribed into cDNA using the QuantiTect Reverse Transcription kit (ThermoFisher Scientific). Gene expression analysis was performed with primers for the reference gene human glyceraldehyde 3-phosphate dehydrogenase *(hGAPDH)*, as well as for the target genes in Table 3. The transcribed cDNA was either mixed with custom-designed primers and the Platinum SYBR Green qPCR SuperMix-UDG kit (Invitrogen), or TaqMan Gene Expression Assays and Fast Advanced Master Mix (Applied Biosystems). Gene expression levels were determined by quantitative polymerase chain reaction (qPCR, QuantStudio 3 real-time PCR system, Applied Biosystems). The melt curves were analysed to confirm the specificity of the reaction and quantification cycle (Cq) 35 cutoff was used. Relative expression levels were calculated using the Cq method ($\Delta Ct = Ct_{(\text{gene of interest})} - Ct_{(GAPDH)}$).

Table 3. Human oligonucleotide primers used for qRT-PCR. Primers with shown sequence were custom designed; primers with assay ID number were purchased from Applied Biosystems. fw: forward; rev: reverse; h: human.

Gene	Sequence (forward and reverse primer)	Product size (bp)
hC3	fw: 5′-TGC TGC CCA GTT TCG AGG TCA-3′ rev: 5′-CCC GTC CAG CAG TAC CTT TCG G-3′	248
hC5	fw: 5′-TGT CGT CGC AAG CCA GCT CC-3′ rev: 5′-TGC CAA TGC CTT GAA TTT CCC AGG-3′	215
hC6	assay ID: Hs01110040_m1	86
hC7	assay ID: Hs00940408_m1	75
hC8A	Assay ID: Hs00175098_m1	76
hC9	assay ID: Hs01036216_g1	84
hCD46	fw: 5′-GTG AGG AGC CAC CAA CAT TT-3′ rev: 5′-GGC GTC ATC TGA GAC AGG T-3′	177
hCD55	fw: 5′- CAG CAC CACCAC AAA TTG AC-3′ rev: 5′-CTG AAC TGT TGG TGG GAC CT-3′	215
hCD59	fw: 5′-CCG CTT GAG GGA AAA TGA G-3′ rev: 5′-CAG AAA TGG AGT CAC CAG CA-3′	130
hGAPDH	assay ID: Hs99999905_m1	122
hIL-6	fw: 5′-AGG AGA CTT GCC TGG TGA AA-3′ rev: 5′-CAG GGG TGG TTA TTG CAT CT-3′	180
hIL-8	fw: 5′-GTG CAG TTT TGC CAA GGA GT-3′ rev: 5′- CTC TGC ACC CAG TTT TCC TT-3′	196
hMMP-1	fw: 5′-ATG CTG AAA CCC TGA AGG TG-3′ rev: 5′-CTG CTT GAC CCT CAG AGA CC-3′	234
hMMP-3	fw: 5′-GGA GAT GCC CAC TTT GAT GAT-3′ rev: 5′-CAT CTT GAG ACA GGC GGA AC-3′	187

Results

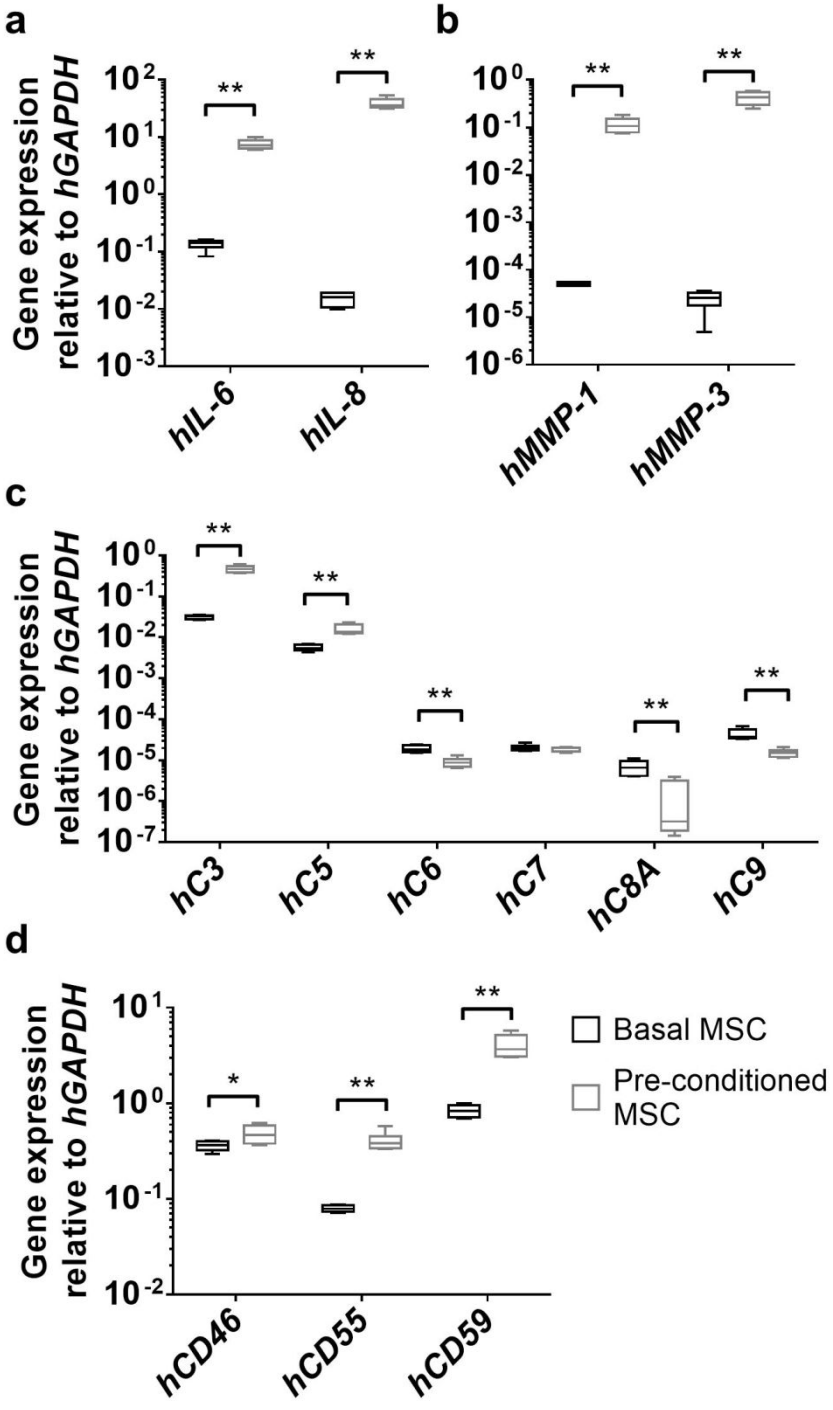

Fig. 9. Gene expression of human MSC after culture under basal (Basal MSC) or preconditioning with 10 ng/mL IL-1β medium supplementation and culture at 37 °C with 6 % O2 and 8.5 % CO2 for 48 h (Pre-conditioned MSC). (**a**) Relative mRNA expression of human pro-inflammatory cytokines *hIL-6*, *hIL-8*, (**b**) matrix metalloproteinases *hMMP-1*, *hMMP-3*, (**c**) complement components *hC3*, *hC5*, *hC6*, *hC7*, *hC8A*, *hC9*, and (**d**) complement inhibitors *hCD46*, *hCD55* and *hCD59*. Results were normalised to expression level of *bGAPDH*. $n = 6$, * $p < 0.05$, ** $p < 0.01$, non-parametric Mann-Whitney test.